Azospirillum brasilense Sp7 and tomato seedling exudate or cytidine reduced disease symptoms on yellow pear tomatoes caused by *Pseudomonas syringae* pv. tomato DC3000

Janice N.A. Tagoe[a], Bidya Ojha[a], Shelley M. Horne[a,] and Birgit M. Prüß[a#]

[a]Department of Microbiological Sciences, North Dakota State University, Fargo, ND, 58108

Running Head: pro-biotic and pre-biotic treatment for tomatoes

#Address correspondence to birgit.pruess@ndsu.edu
Department of Microbiological Sciences Dept. 7690
North Dakota State University
Fargo, ND 58108-6050
(701) 306-6913

Abstract

Tomatoes are an important crop worldwide and phytopathogens can cause devastating losses. Our study describes a combination treatment for tomatoes, consisting of pro-biotic *Azospirillum brasilense* Sp7 and either complete tomato seedling exudate or the single exudate compound cytidine. The combination of *A. brasilense* Sp7 with cytidine showed a remarkable reduction of 83.4% in disease symptoms of the tomatoes that had been challenged with *Pseudomonas syringae* pv. tomato DC3000. Replacing cytidine with tomato seedling exudate was slightly less

effective at 71%, but the reduction in disease symptoms was still larger than with *A. brasilense* Sp7 alone at 55%. This reduction in disease symptoms was not paralleled by a reduction in *Pseudomonas* live counts, abundance of *P. syringae* pv. tomato DC3000 16S rDNA, or copies of the *P. syringae hrpL* gene in leaf homogenates. The symptom reduction was paralleled by a 6.7 fold increase in *A. brasilense* Sp7 16S rDNA in root homogenates in response to germinating the seeds in cytidine. In the phyllosphere, bacterial 16S rDNA could only be detected in leaf homogenates from plants that were challenged with *P. syringe* pv. tomato DC3000. In phyllosphere and rhizosphere, treatments modulated the microbiome. At the species level, *A. brasilense* together with cytidine reduced the presence of *Stenotrophomonas maltophilia*, a human pathogen, in the phyllosphere. In the rhizosphere, adding *A. brasilense* Sp7 might have caused a switch from Rhizobiales to Azospirillales.

Importance (145 words)

The importance of the study is two-fold. First, *P. syringae* pv. tomato reduces crop yield of tomatoes; symptoms of infection include dark brown leaf lesions, wilting, and ultimately death of the leaf and then the plant. Our combination treatments appear to be an effective tool to reduce disease symptoms upon infection with *P. syringae* pv. tomato. Second, *P. syringae* pv. tomato is a model system to study the molecular mechanism of host responses to phytopathogens on tomatoes (1). The tri-partite system consisting of *A. brasilense*, *P. syringae* pv. tomato DC3000, and tomatoes is the basis for our phytopathogen experiments and used as a model system in our study. Since *A. brasilense* is a generalist with a wide range of hosts, we anticipate that our combination treatments will, in similar compositions of bacteria and seed exudate compounds, help to protect other plants against their respective phytopathogens.

Introduction

Tomatoes (*Solanum lycopersicum*) are considered specialty crop, as well as emerging crop in North Dakota that are primarily grown in greenhouses and on Community Supported Agriculture farms. Worldwide, tomatoes are an economically very important vegetable crop (2). Crop losses can occur through infections by phytopathogens, which can be both fungal (*e.g. Fusarium oxysporum* f. sp. *lycopersici* (3)) or bacterial (*e.g. Pseudomonas syringae* pv. tomato (4)). The latter pathogen has been used as a model organism for the understanding of phytopathogen infection in tomatoes since the 1980s. The commonly used *P. syringae* pv. tomato DC3000 was isolated in 1991 from *Arabidopsis thaliana* (5). The first step towards colonization and infection is bacterial chemotaxis towards plant exuded metabolic intermediates. These include amino acids such as GABA and L-proline (6), as well as L-aspartate, L-glutamate, and D-aspartate via the PsPto-PscC chemoreceptor on the pathogen (7). Infection of the apoplast includes a type III secretion system and suppression of the plant immune system (8).

Protection of tomatoes against their phytopathogens can be mediated by natural components of the soil microflora referred to as Plant Growth Promoting Rhizobacteria (PGPR). This includes other species of *Pseudomonas*, such as *Pseudomonas resinovorans*, *Pseudomonas vranovensis*, or *Pseudomonas putida* (9). *Azospirillum brasilense* is currently recognized as a PGPR whose benefits far exceed its metabolic capabilities. Originally identified as forming associations with wheat (*Tritivum aestivum*, (10)) and maize (*Zea mays*, (11)), it's uses have extended to a variety of fruits and vegetables, including tomatoes (12). After seed inoculation, *A. brasilense* caused genetic and physiological changes of the phyllosphere and rhizosphere of cherry tomatoes (13). The PGPR can colonize many different plant tissues, such as roots of maize (14) or leaves of tomatoes (15). In the association model by Bashan and De-Bashan (16),

colonization by *A. brasilense* Cd was investigated in roots and on leaves. Disease symptoms caused by *P. syringae* pv. tomato DC3000 were reduced in the presence of the PGPR.

The rhizospheric lifestyle of *A. brasilense* relies on multiple mechanisms for efficient niche colonization, including motility and chemotaxis towards plant root or seed exuded metabolic intermediates, aggregation and biofilm formation, phytohormone production, and cell to cell communication (17). Several chemoreceptors (*e.g.* AerC, Tlp4b, Tlp2) and the histidine kinases CheA1 and CheA4 start a signaling system that responds to a variety of chemoattractants, including nitrate and nitrite, connects to nitrogen metabolism, and facilitates root colonization (18-20). Intriguingly, movement of *A. brasilense* across a gradient of chemicals has been described more generally as energy taxis, where the bacteria move towards attractants that increase their intracellular energy (21). In agreement with this, our own research showed migratory behavior for *A. brasilense* on semi solid swim plates containing any of 15 compounds tested that had been identified in seedling exudates of tomatoes, peas, or cucumbers (22). The same study also described tomato seedling exudate as a near perfect medium for growth and migration of *A. brasilense* (22).

With this study, we tested the hypothesis that tomato seedling exudate might enhance the ability of *A. brasilense* Sp7 to aid the tomato plants in resisting infection with *P. syringae* pv. tomato DC3000. We used the experimental protocol by the Filiatrault lab (23), where tomatoes grown for 4 weeks got challenged with *P. syringae* pv. tomato DC3000. The protocol was modified by germinating seeds in tomato seedling exudate or the single exudate compound cytidine and adding *A. brasilense* Sp7 at the time of planting. In an extension to the tri-partite model of PGPR, pathogen, and tomato, we looked at the plants as a meta-organism and investigated the effect of the treatments on phyllosphere and rhizosphere of the tomatoes.

Results

Combination treatment *of A. brasilense* Sp7 with tomato seedling exudate or cytidine decreased disease symptoms on yellow pear tomatoes after challenge with *P. syringae* pv. tomato DC3000

The phytopathogen experiment was done in 12 test groups, covering absence or presence of each of the following: *A. brasilense* Sp7 (*Abra*), *P. syringae* pv. tomato DC3000 (Ps), seedling exudate (Ex), or cytidine (CYD). Fig. 1 shows the disease symptoms at 5 to 7 days post challenge with the pathogen from 3 to 4 replicate experiments and 3 to 6 plants per test group.

The *p*-value from the one-way ANOVA across the 12 test groups was <0.0001. This was also the *p*-values from the Tukey pairwise comparisons for the six comparisons between plants challenged or not challenged with *P. syringae* pv. tomato DC3000 (*p*-values not included in Fig. 1). There were almost no disease symptoms in the absence of the pathogen (white bars). For the three comparisons between plants inoculated or un-inoculated with *A. brasilense* Sp7 (-*Abra* +Ps versus +*Abra* +Ps; -*Abra* +Ex +Ps versus +Abra +Ex +Ps; -*Abra* +CYD +Ps versus +*Abra* +CYD +Ps) (*p*-values in purple), the *p*-values were <0.0001, 0.0023, and <0.0001, respectively. *A. brasilense* Sp7 had a positive effect on the health of the challenged plants. The -*Abra* +Ps vs +Abra +Ps comparison yielded a moderate reduction in disease symptoms of only 55%.

An improvement was accomplishment by germinating the seeds in cytidine (*p*-values in green). Comparing the test group -*Abra* +Ps to the test group +*Abra* +Cyd +Ps, the reduction in disease symptoms was 83.4% at a *p*-value of <0.0001. The test group +*Abra* +Ps was still different from the test group +*Abra* +Cyd +Ps with a *p*-value of 0.0117 and a reduction of 63.2%. In the presence of *A. brasilense* Sp7, cytidine was able to cause further reduction in disease symptoms. The largest reduction relative to the -*Abra* +Ps group can be accomplished by

adding both, the PGPR and the tomato seedling exudate compound cytidine. In the absence of *A. brasilense* Sp7, cytidine did not reproducibly decrease disease symptoms.

Seedling exudate was less effective at reducing disease symptoms (*p*-values in red). Between +*Abra* +Ps and +*Abra* +Ex +Ps, there was a 35% reduction in disease symptoms. However, the *p*-value did not indicate a statistical significance of the difference between the two test groups. Comparing the test group -*Abra* +Ps to the test group +*Abra* +Ex +Ps, the reduction in disease symptoms was 71% at a *p*-value of <0.0001. The combination of *A. brasilense* Sp7 and seedling exudate was effective at reducing disease, but less effective than the combination of *A. brasilense* Sp7 and cytidine. In summary, *A. brasilense* Sp7 partially reduced disease symptoms, the reduction could be enhanced by germinating seeds in seedling exudate and more so in cytidine.

None of the disease symptom reducing treatments reduced *Pseudomonas* counts on the phytopathogen challenged tomato leaves

To determine whether the reduction in disease symptoms caused by the combination treatment was paralleled by a reduction in live counts of bacteria from the genus *Pseudomonas*, we homogenized leaf samples from three phytopathogen experiments, serially diluted the homogenates, and plated onto King's B medium, supplemented with rifampicin. Fig. 2 shows the $\log_{10}$ CFU/g data from the colony counts.

The *p*-value from the one-way ANOVA that compared all test groups was <0.0001. The only statistically significant differences from the pairwise comparisons were five out of six comparisons where a test group of plants challenged with *P. syringae* pv. tomato DC3000 was compared to a group that did not get challenged (*e.g.* -*Abra* +Ps versus -*Abra* -Ps). The sole exception was the comparison of the test groups +*Abra* +Ex +Ps versus +*Abra* +Ex -Ps, which

yielded a *p*-value from the Tukey pairwise comparison of 0.0509. Plants challenged with the pathogen contained a mean between 8.1 and 9.25 $\log_{10}$ CFU of *Pseudomonas*/g of plant material (red bars). Unchallenged plants contained a smaller but still remarkable number of *Pseudomonas* between 4.2 and 7.2 $\log_{10}$ CFU/g (white bars). A second ANOVA was performed to compare all test groups of plants that had been challenged with the pathogen. The *p*-value for this comparison was 0.2012, indicating there were no statistically significant differences between plants that were challenged with *P. syringae* pv. DC3000. The difference in disease symptoms caused by *A. brasilense* Sp7 in combination with seedling exudate or cytidine was not paralleled by a reduction of the *Pseudomonas* count on the leaves.

None of the disease symptom reducing treatments reduced the abundance of *P. syringae* pv. tomato DC3000 16S rDNA or copies of the *hrpL* gene within the phyllosphere of phytopathogen challenged tomatoes

To confirm the data from the *Pseudomonas* count with *P. syringae* pv. tomato DC3000 16S rDNA, homogenates were produced from the same experiment, but different leaf samples. DNA was isolated from the homogenates and 16S rDNA was sequenced. For the complete abundance table, please, see Supplemental Table 1. The *P. syringae* DC3000 tab in Supplemental Table 1 contains 1 row with data from *P. syringae* pv. tomato DC3000 from AB001445.1.1538, the tomato tab contains 15 rows of data from species of the *Solanum* genus. Fig. 3 shows the results for the *P. syringae* and tomato analysis.

In Fig. 3A, we plotted the *P. syringae* pv. tomato DC3000 abundances (left) and tomato abundances (right) separately. The *p*-value from the one-way ANOVA that was performed on the *P. syringae pv.* tomato DC3000 data was 0.0177, indicating statistically significant differences between some of the test groups. However, calculating an ANOVA across only the test groups of

plants that had been inoculated with *P. syringae* pv. tomato DC3000 was 0.1740. The only statistically significant differences were between test groups whose sole treatment difference was presence or absence of the pathogen. Leaf homogenates from tomato plants that did not get challenged with *P. syringae* pv. tomato DC3000 did not contain 16S rDNA from the challenge pathogen. The *p*-value from the one-way ANOVA that was performed on the tomato abundances was 0.5804, failing to indicate statistically significant differences between these data. This implies that the difference between the pathogen challenged and unchallenged test groups of plants was not due to differences in the amounts of DNA used for 16S rDNA sequencing. Our disease symptom reducing treatments did not reduce the abundance of *P. syringae* pv. tomato DC3000 16S rDNA on the leaves.

As final confirmation that our treatments did not alter the amount of *P. syringae* pv. tomato DC3000 on the leaves, we performed digital PCR, using the same DNA samples. Fig. 3B shows big differences in copies of the *hrpL* gene between test groups that were challenged with the pathogen and those that were not (red vs white bars). The ANOVA that was computed across all 12 test groups did point towards statistically significant differences with a *p*-value of 0.0082. However, calculating an ANOVA across only the test groups of plants that had been inoculated with *P. syringae* pv. tomato DC3000 was 0.1157. Our treatments did not reduce the copy numbers of the *P. syringae* pv. tomato DC3000 *hrpL* gene. This increases our confidence that the treatments did not impact the amount of the challenge pathogen on the leaves.

Cytidine increased the abundance of 16S rDNA from *A. brasilense* Sp7 in the rhizosphere

Since we were unable to detect 16S rDNA from *A. brasilense* Sp7 in leaf homogenates, we determined the effect of the combination treatment on colonization by *A. brasilense* Sp7 within the rhizosphere. For the complete abundance table from the 16S rDNA analysis of the

root homogenates, please, see Supplemental Table 2. The *A. bra* tab contains one row with *A. brasilense* data from *Azospirillum brasilense* AF533354.1.1439. Fig. 4 shows the results for the *A. brasilense* Sp7 analysis. The ANOVA that was performed on the complete data set yielded a *p*-value of 0.0779, all pairwise comparisons were also non-significant. However, performing two additional pairwise comparisons yielded *p*-values of statistical significance, namely from the comparison between +*Abra* -Ps versus +*Abra* +CYD -Ps. Cytidine increased 16S rDNA abundance for *A. brasilense* Sp7 by 6.7 fold with *p*-values of 0.0004 and 0.05 from the parametric *t*-test and the non-parametric Mann-Whitney U test, respectively.

A. brasilense Sp7, seedling exudate, and cytidine modulated the phyllosphere of phytopathogen challenged tomatoes

The first analysis from the phyllosphere was to compute a phylogenetic tree from the 67 taxonomies that produced relative abundances of 16S rDNA larger than 50 summed across all 12 test groups (Fig. 5). The data clustered into two phyla, Proteobacteria and Bacteroidota. There are 5 species of Sphingomonadales (purple) and 5 species of Rhizobiales (green) among the Alphaproteobacteria, 3 species of Burkholderiales (brown) from the Betaproteobacteria, as well as 2 species of Xanthomonadales (dark purple), 24 species of Pseudomonadales (blue), and 28 species of Enterobacteria (orange) among the Gammaproteobacteria. The order Enterobacterales included the families of *Erwiniaceae* and *Enterobacteriaceae*, the Pseudomonadales were all from the family *Pseudomonadaceae* and the genus *Pseudomonas*. The two species of Bacteroidota were *Flavobacterium ginsengiterrae* from the order Flavobacteriales (yellow) and *Pedobacter kyungeensis* from the order Sphingobacteriales (red). Overall, our leaf homogenates included predominantly species from the Proteobacteria clustered to six different bacterial orders, as well as two species/orders of Bacteroidota.

The following two analyses considered alpha diversity (Fig. 6A) and 16S rDNA abundances (Fig. 6B), computed separately for each of the 3 replicates for the 12 test groups from all 67 taxonomies within the phyllosphere. Both, the alpha diversity Shannon index for richness (Fig. 6A) and the sum abundances across all taxonomies from each test group (Fig. 6B) pointed towards a more or less complete lack of 16S rDNA within the phyllosphere of tomatoes that had not been challenged with *P. syringae* pv. tomato DC3000. For the sum abundances (Fig. 6B), the *p*-value from the one-way ANOVA pointed towards a lack of statistical significance of this difference. For alpha diversity (Fig. 6A), five out of six comparisons between test groups whose only treatment difference was challenge or no challenge with the pathogen had a *p*-value below 0.05. By all appearances, the presence of the pathogen permits rise to a myriad of bacteria. Among the test groups that had been challenged with the pathogen, the group +*Abra* +Ex +Ps exhibited both a low Shannon index, as well as low sum abundance. The test groups -*Abra* + Ps and +*Abra* +CYD +Ps also had low sum abundances across the 67 phyllosphere taxonomies (Fig. 6B).

Fig. 6C visualizes the percentage of 16S rDNA abundances that were summed across all taxonomies from each of the 8 orders as a heatmap. This was done solely for test groups that had been challenged with the pathogen. Enterobacterales scored highest at 67.9% for the +*Abra* +Ex +Ps test group. The second highest percentage of Enterobacterales was observed for the +*Abra* +Ps test group at 36.92%. Pseudomonadales scored highest at 78.7% for the +*Abra* +CYD +PS test group. Xanthomonadales had a 13.32% abundance in the -*Abra* +Ps group. Xanthomonadales were also moderately high at 10.58% in the -*Abra* +Cyd +Ps group. Most remarkably, the abundance of Xanthomonadales was reduced by *A. brasilense* Sp7 in all three comparisons that compared a test group with *A. brasilense* Sp7 inoculated tomato plants to a test

group with un-inoculated plants (*e.g.* -*Abra* +Ps vs +*Abra* +Ps). Note that *Stenotrophomonas maltophilia* was one out of two species in this order and the only species that had a respectable abundance (Supplemental Table 1).

Associations between 16S rDNA from test groups and bacterial orders were computed with principal component analysis (PCA) from the mean of the percent abundances from the 6 test groups that had been challenged with the pathogen (Figs. 6D and E). PC1 captured 66% of the total variation and PC2 captured an additional 25.09% to a cumulative coverage of 91.08%. Three other components were computed, contributing 5.32%, 3.4%, and 0.2% to the coverage. The 6 treatments grouped distinctly within the PC space, implying strong multivariate separation between treatments (Fig. 6D). The furthest outlier appeared to be the +*Abra* +Ex +Ps group (yellow) with the PC1 coordinate 2.71 and the PC2 coordinate -2.091. Enterobacterales associated strongly with this +*Abra* +Ex +Ps test group (yellow) in the biplot (Fig. 6E) with a cosinus similarity of 0.924. Pseudomonadales associated strongly with the +*Abra* +CYD +Ps with a cosinus similarity of 0.998 and moderately with the -*Abra* +CYD +PS test group with a cosinus similarity of 0.836 (both light blue in Fig. 6D and E).

A. brasilense Sp7, seedling exudate, and cytidine impacted the rhizosphere of phytopathogen challenged tomatoes

Data from Supplemental Table 2 were analyzed in a way that was similar to the phyllosphere. The first analysis from the rhizosphere was to compute the phylogenetic tree from the 102 taxonomies that produced relative abundances of 16S rDNA equal to or larger than 500 combined across all 12 test groups and did not belong to the Proteobacteria (Fig. 7). These taxonomies separated into eight different phyla, Bacteroidota, Actinobacteriota, Abditibacteriota, Bdellovibrionata, Myxococcota, Planctomycetota, Acidobacteriota, and Patescibacteria. By far

the largest group were the Bacteroidota with 62 species of bacteria (green), belonging to the bacterial orders of Chitinophagales, Cytophagales, Flavobacteriales, and Sphingobacteriales. The second largest group were the Actinobacteriota with 19 representative bacterial species (light blue), belonging to the bacterial orders Actinobacterales, Frankiales, Propionibacteriales, Micrococcales, and Microtrichales.

Not presented in the phylogenetic tree are 93 taxonomies of Alphaproteobacteria, 42 taxonomies of Betaproteobacteria, and 43 taxonomies of Gammaproteobacteria (Supplemental Table 2). The Alphaproteobacteria clustered into seven bacterial orders, Acetobacterales, Azospirillales, Caulobacteriales, Micropepsales, Rhizobiales, Rhodospirillales, and Sphingomonadales. The Betaproteobacteria were solely represented by members of the Burkholderiales. Gammaproteobacteria were Enterobacterales, Pseudomonadales, Salinisphaerales, and Xanthomonadales.

Alpha diversity (Fig. 8A) and 16S rDNA abundances (Fig. 8B) were computed separately for each of the 3 replicates for the 12 test groups from all 280 taxonomies within the rhizosphere. Both, the alpha diversity Shannon index for richness (Fig. 8A) and the sum abundances across all taxonomies from each test group (Fig. 8B) showed 16S rDNA within the rhizosphere of all twelve test groups of plants. For alpha diversity, there was little variation between the test groups, with the possible exception of the +*Abra* -Ps test group. For 16S rDNA abundances, there was some degree of fluctuation. However, the *p*-value from the one-way ANOVAs for both analyses pointed towards a lack of statistical significance of any differences.

Fig. 8C shows the percentage of 16S rDNA abundances that were summed across all taxonomies from each of the 29 bacterial orders as a heatmap. Rhizobiales were very high in the -*Abra* -Ps group at 30.85%, in the +*Abra* -Ps group at 28.59%, the -*Abra* +Ex +Ps group at

27.27%, the -*Abra* +Ex -Ps group at 25.52%, and the -*Abra* +CYD -PS group at 24.5%. Pseudomonadales were high (>24%) in the -*Abra* +Ps, -*Abra* +Ex +Ps, -*Abra* +CYD +Ps and -*Abra* +CYD -Ps groups and lower in the +*Abra* groups. Burkholderiales had the highest percent abundance among any bacterial orders in the +*Abra* +Ps group at 32.9%. In the +*Abra* +Ex +Ps group, Burkholderiales were still high at 28.46%. Flavobacteriales were high in the -*Abra* -Ps group at 23.55%, the -*Abra* +Ex +Ps group at 25.05%, and the -*Abra* +CYD +Ps group at 24.15%. Bacteriovoracales were high in the -*Abra* +Ex –Ps group at 21.04%.

Fig. 9 shows the results from the PCA that was computed from the mean of the percent abundances from all 12 test groups. In Figs. 9A and 9B, PC1 captured 35.65% of the total variation and PC2 captured an additional 15.05% to a cumulative coverage of 50.7%. Nine other components were computed. Treatments with "+A" resembling the presence of *A. brasilense* Sp7 clustered on the left side of the y-axis, while treatments designated "-A" resembling the absence of the inoculant clustered on the right side (Fig. 9A). This suggests that PC1 was strongly influenced by the presence or absence of the PGPR. In the bottom right hand quadrant of Fig. 9B, (PC1 +, PC2 -), Micrococcales associated strongly with the test group +*Abra* +CYD -Ps (+A +C -P) at an association strength of 0.995, Sphingobacteriales, Azospirillales, and Salinisphaerales pointed into the direction of the same test group with moderate association strengths of 0.921, 0.919, and 0.927, respectively. In the bottom left hand quadrant (PC1 -, PC2 -), Flavobacteriales associated strongly with the -*Abra* +Ex +Ps (-A +E +P) test group with a cosinus similarity of 0.993 and moderately with the -Abra +CYD +Ps (-A +C +P) test group with a cosinus similarity of 0.932. Pseudomonadales associated strongly with the -*Abra* +Ps (-A +P) and the -*Abra* +CYD +Ps (-A +C +P) groups at association strengths of 0.965 and 1, respectively. Cytophagales, Gemmatales, and Polyangales were also in this quadrant, but with

weak associations. In the upper left hand quadrant (PC1 -, PC2 +), Propionibacteriales and Saccharomonadales associated strongly with the -*Abra* +CYD -Ps (-A +C -P) test group with association strengths of 0.981 and 0.998, respectively. Rhizobiales, Tepidisphaerales, and Abditibacterales associated extremely strongly with the -*Abra* +Ps (-A +P) test group (1, 1, 0.999, respectively). In the upper right hand quadrant (PC1 +, PC2 +), weak associations could be noted between Microtrichales and the +*Abra* +Ex +Ps (+A +E +P) and +*Abra* +Ex -Ps (+A +E -P) test groups (0.892 and 0.875).

Altogether, Micrococcales, Sphingomonadales, Azospirillales, Salinisphaerales, and Microtrichales associated positively with the presence of *A. brasilense* Sp7. Flavobacteriales, Pseudomonadales, Propionibacteriales, Saccharomonadales, Rhizobiales, Tepidisphaerales, and Abditibacterales associated positively with the absence of *A. brasilense* Sp7.

As a final analysis of the rhizosphere, we focused on the inverse effect that inoculation with *A. brasilense* Sp7 exhibited on two orders of PGPR, Azospirillales and Rhizobiales. We used the 16S rDNA abundances for those two bacterial orders across the twelve test groups (Fig. 10). The abundances of Rhizobiales were approximately 20 fold higher than that of Azospirillales. There was a general tendency for test groups that contained plants inoculated with *A. brasilense* Sp7 to contain more Azospirillales than test groups containing un-inoculated plants, while these same test groups contained a lower abundance of Rhizobiales. The *p*-values from the two-way ANOVA were 0.0556 for test groups and <0.0001 for bacterial orders. The Tukey *post hoc* test yielded four comparisons that produced a *p*-value below 0.05. For each of these comparisons, Rhizobiales were reduced in the presence of the inoculant. We observe that inoculation of tomatoes with *A. brasilense* Sp7 is paralleled by a switch from Rhizobiales to Azospirillales in the rhizosphere.

Discussion

Altogether, our combination treatment of pro-biotic *A. brasilense* Sp7 and pre-biotic tomato seedling exudate or the single exudate compound cytidine reduced disease symptoms of tomatoes after challenge with *P. syringae* pv. tomato DC3000. This effect was larger for the treatment that included cytidine than the one including total exudate. The reduction in disease symptoms was not paralleled by a reduction in the live *Pseudomonas* counts or the abundance of *P. syringae* pv. tomato DC3000 16S rDNA on the leaves. It is possible that there was an increase in root colonization of *A. brasilense* Sp7 in response to germinating the seeds in cytidine. Both phyllosphere and rhizosphere underwent multiple changes in response to the treatments.

Phytopathogen resistance

P. syringae pv. tomato DC3000 has long been used to model infectious disease in plants (8, 23-27), infection requires motility and a type III secretion system (6, 7, 9, 28). The backbone of our phytopathogen experiments are the studies by the laboratories of Dr. Emilia Lopez-Solanilla (7) and Dr. Melanie Filiatrault (23); the original protocol was modified by the supplementation with cytidine or total seedling exudate in the germination step and *A. brasilense* Sp7 at planting.

In our phytopathogen experiment, *A. brasilense* Sp7 alone reduced disease symptoms caused by *P. syringae* pv. tomato DC3000 by 55%, while the combination treatment of *A. brasilense* Sp7 and cytidine reduced disease symptoms by 83.4% (Fig. 1). The latter plants looked very similar to plants that had not been challenged with the pathogen. The combination treatment of *A. brasilense* Sp7 and total seedling exudate was less effective at 71% reduction in disease symptoms (Fig. 1).

After we observed this disease reduction, we asked whether our treatments would decrease the number of our challenge bacteria *P. syringae* pv. tomato DC3000 on the tomato leaves. According to the *Pseudomonas* counts, *P. syringae* pv. tomato DC3000 16S rDNA analysis of the leaf homogenates, and dPCR targeting the *P. syringae* specific transcriptional regulator HrpL (29), this was not the case (Figs. 2 and 3). It is noteworthy that live *Pseudomonas* counts were still quite high in plants that had not been challenged with the pathogen at 4.2 to 7.2 CFU/g. This is because King's B medium does not just detect *P. syringae*, but a range of species from the genus *Pseudomonas* (30).

The next question was whether the treatments would enhance colonization of phyllosphere or rhizosphere by our inoculant *A. brasilense* Sp7. The phyllosphere did not contain any detectable abundance of *A. brasilense* Sp7 16S rDNA. In the rhizosphere, colonization by *A. brasilense* Sp7 might have been enhanced by cytidine, as evidenced by 16S rDNS (Fig. 4). We did perform digital PCR on the inoculant PGPR as well, but could not detect any copies of the sequence-characterized amplified region (SCAR) markers that are characteristic for *Azospirillum* (31) in any of the samples. We conclude that cytidine does not decrease disease symptoms by decreasing abundance of *P. syringae* pv. tomato DC3000 in the phyllosphere. It is possible that cytidine enhances colonization of the rhizosphere by *A. brasilense* Sp7.

The suppression of disease symptoms by rhizobial bacteria is consistent with work by Yin *et al.* (32) who found a reduction of *Ralstonia solanacearum* by *Sphingomonas* sp. and *Pseudomonas putida*, as well as Huang and coworkers (33) who worked with a community of *Asticcacaulis* sp., *Arachidicoccus* sp., and *Phenylobacterium* sp to enhanced oxylipin pathways in infected tomato leaves and prevent gray mold disease. A study with tobacco (*Nicotiana tabacco*) inoculated with *Phytophthora nicotianae* found that the plant exudate compound

methyl ferulate inhibited *P. nicotianae* and prevented tobacco black shank disease (34). A study with *A. brasilense* as inoculant and *Pseudomonas protegens* as pathogen found that plant exuded benzoxazinoids stimulated chemotaxis for the inoculant, but not for the pathogen (35). We believe that our data contribute to the growing body of evidence that seedling exudate compounds together with PGPR can help crop plants resist phytopathogens.

Phyllosphere and rhizosphere

To extend the perspective from looking at the experiment as a tri-partite relationship between two bacterial and one plant species to viewing the tomatoes as one meta-organism, we wanted to know how our disease reducing treatments might impact tomato phyllosphere and rhizosphere. Comparing the microbiome of leaves to that of roots, a first noticeable difference was the almost complete lack of 16S rDNA from any bacteria in leaf homogenates from tomatoes that had not been challenged with *P. syringae pv.* tomato DC3000 (Fig. 6A and B). In root homogenates, we detected 16S rDNA from a similar number of bacterial species (Fig. 8A) at similar abundances (Fig. 8B) across all 12 test groups. A second large difference between phyllosphere and rhizosphere was alpha diversity. In the phyllosphere, we started with 684 taxonomies, which were narrowed down to 67 after applying the $\geq$50 filter. In the rhizosphere, we initially obtained 8,619 taxonomies, which we narrowed down to 280, applying the much more restrictive $\geq$500 filter. As one similarity between the two microbiomes, Proteobacteria were the pre-dominant phylum in both, though at different percentages from the total.

In the phyllosphere, the percentage of Proteobacteria species from the total number of species was 97.1%. The only exceptions were two species from the phylum Bacteroidota. This is consistent with current literature, reporting Proteobacteria as the most abundant phylum in the tomato microbiome (36). Within this phylum, 84% of the species belong to the

Gammaproteobacteria (37), especially of the genera *Acinetobacter*, *Pseudomonas*, and *Enterobacter* (36). In agreement with this, our experiments identified Enterobacterales as the predominant order on leaves with 28 taxonomies and Pseudomonadales with 24 (Fig. 5).

In the rhizosphere, the percentage of Proteobacteria from the total number of species was 64%. In addition, we found Bacteroidota, Actinobacteriota, Abditibacteriota, Bdellovibrionota, Mycococcota, Planctomycetota, Acidobacteriota, and Patescibacteria (Fig. 7). Of these, Actinobacteriota, Bacteroidota, Verrucomicrobiota, and Patescibacteria have been identified as tomato endophytes in the roots previously alongside Proteobacteria (38). This previous study also found Firmicutes, which we failed to identify. Intriguingly, a decrease in Actinobacteria and Firmicutes abundance in the rhizosphere increased susceptibility to disease in one study (39). Another group found Rhizobiales and Myxococcales (40), both of which were identified as part of the rhizosphere in our experiment (Fig. 7). The high richness and diversity in our rhizosphere is consistent with results from a comparative study on tomato phyllosphere, rhizosphere, and endophytic roots, which also found Proteobacteria to be the dominant phylum (36). These researchers found high levels of Pseudomonas and Acinetobacter in the rhizosphere. Most Pseudomonadales which scored high abundances in our experiment were from the genus *Pseudomonas*. Further at the genus level, *Sphingobium* has been described frequently. It is enriched in the rhizosphere in response to α-tomatin (41), produces indole 3-acetic acid (42), and catalyzes toxic steroidal glycoalkaloids (43). *Sphingobium* had by far the largest abundance of 16S rDNA in our rhizosphere experiment among the Sphingomonadales.

Plant exudates and the plant microbiome

The connection between plant exuded metabolic intermediates and the plant microbiome is not a new recognition. Tomatoes are capable of exuding a wide array of metabolic

intermediates into the soil to promote their own health and disease resistance. This includes several compounds that our own previous study did not look for (22), such as α-tomatin, solanacol, and methyl salicylate (44, 45). Disease suppression can even include intercropping systems, where intercropping of tomatoes or potatoes with onions added *Bacillus* sp. to the tomato rhizosphere, effectively suppressing leaf wilt caused by the soil bacteria *Verticillium dahlia* (46). Additionally, bacteria of the genus *Bacillus* triggered the release of acylsugars into the soil (47). A study with a different PGPR targeted the rhizosphere of tomatoes challenged with *Ralstonia solanacearum* for metabolites (48). These researchers identified ribose, lactic acid, and xylose, among others, to be used by the beneficial rhizospheric bacteria, but not by the pathogen (48). At a concentration of 1 µmol/g applied to the soil, these metabolites protected the tomato plants from pathogens (48). A recent review article summarized exudates as a bridge between roots and rhizospheric microbes (49). As one example, xanthine was exuded by roots of salt stressed soybeans (*Glycine max*) and enriched the rhizospheric microbiome, especially by the bacteria of the genus *Pseudomonas* that aided the plants in resisting salt stress (50). A second example came from tomatoes, where the two root exudate compounds riboflavin and 3-hydroxyflavone improved plant resistance against *R. solanacearum* (51). This included the recruitment of bacteria from the genus *Streptomyces* (51).

Analyzing 16S rDNA abundances within our phyllosphere, the genera Enterobacterales, Pseudomonadales, and possibly Xanthomonadales were impacted by different combination treatments with *A. brasilense* Sp7, tomato seedling exudate, and cytidine. Enterobacterales were represented at 67.9% within the phyllosphere of tomato plants of the treatment group +*Abra* +Ex +Ps in the heatmap of Fig. 6C. In the PCA analysis of Figs. 6D and E, we see an association of Enterobacterales with the same treatment, +*Abra* +Ex +Ps. Pseudomonadales were represented at

74.7%, 68.2%, and 78.7% in the test groups -*Abra* +Ex +Ps, -*Abra* +CYD +Ps, and +*Abra* +CYD +Ps, respectively (Fig. 6C). In the PCA analysis of Figs. 6D and E, Pseudomonadales associated with both two cytidine containing test groups. In the heatmap of Fig. 6C, Xanthomonadales were represented at more than 10% in the phyllosphere of tomatoes of the treatment groups -Abra +PS and -*Abra* +Cyd +Ps. However, the PCA analysis from Figs. 6D and E failed to detect an association of this bacterial order with any of the test groups.

In summary from the phyllosphere, there are three distinct outcomes of our treatments on specific bacterial orders; first, tomato seedling exudate increased the abundance of Enterobacterales in the presence of *A. brasilense* Sp7. Second, cytidine increased the abundance of Pseudomonadales, more so in the presence of *A. brasilense* Sp7. Third, there is a possibility that *A. brasilense* Sp7 decreased the abundance of Xanthomonadales in all three comparisons between a -*Abra* and a +*Abra* test group.

Members of the Xanthomonadales are often phytopathogens for a large variety of crop plants, causing devastating crop losses. A recent review article suggests the use of microorganisms for control instead of chemicals (52). In our study, *Stenotrophomonas maltophilia* is the only one of two taxonomies in the Xanthomonadales that yielded a significant abundance of 16S rDNA. *S. maltophilia* is not a phytopathogen, but a PBPR that protects tomatoes against southern blight disease caused by *Sclerotium rolfsii* (53). It is, however, a human pathogen, causing a number of respiratory, bloodstream, and urinary tract infections (54). Comparing the treatment groups -*Abra* +CYD +Ps and +*Abra* +CYD +Ps, inoculation with *A. brasilen*se Sp7 decreased abundance of *S. maltophilia* 16S rDNA by a factor of 7.6.

A second human pathogen in our data set comes from the amplicon sequence variant (ASU) from the unidentified HL756478.3.1418 among the Enterobacterales. This ASU had

100% identity with *Enterobacter cloaceae* (Supplemental Table 3). *E. cloacae* is a phytopathogen causing brown necrosis on tomato leaves (55). It is also a human pathogen, causing gastrointestinal infections, endocarditis and meningitis (56). This species has by far the highest abundance of 16S rDNA among the Enterobacterales (Supplemental Table 1). Intriguingly, it is the rhizosphere that has long been described as a reservoir for human pathogens, including those of the genera *Enterobacter* and *Stenotrophomonas* (54, 57). Kim and coworkers described this transfer of human pathogens from plants as 'crossing the kingdom border' (58). In our experiments, we detected *E. cloaceae* and *S. maltophilia* in the phyllosphere. We hypothesize that our environment friendly treatments may have an impact on public health and food safety in addition to supporting plant health and phytopathogen resistance.

Analyzing 16S rDNA abundance within the rhizosphere, absence or presence of *A. brasilense* Sp7 appeared to be the largest driver behind the PC1 component (Fig. 9A). Comparing data from the heatmap to those from the PCA analysis, we see a shift from Flavobacteriales, Pseudomonadales, Propionibacteriales, Saccharomonadales, Rhizobiales, Tepidisphaerales, and Abditibacteriales in the absence of the PGPR to Micrococcales, Sphingomonadales, Azospirillales, Salinisphaerales, and Microtrichales in the presence of *A. brasilense* Sp7 (Figs. 8C and 9B).

A striking observation is that our inoculant appears to increase the abundance of members of its own order, Azospirillales. To our knowledge, this has not been described before. Another large group of PGPR, Rhizobiales, was decreased in the presence of the inoculant. To further investigate the inverse effect of the inoculant on Azospirillales and Rhizobiales, we graphed the 16S rDNA abundances for the two bacterial orders across all test groups (Fig. 10). Four pairwise comparisons between test groups yielded *p*-values below 0.05. All these came

from the Rhizobiales and the test group of plants that had been inoculated with *A. brasilense* Sp7 had a lower abundance of Rhizobiales than the un-inoculated test group. Our inoculant appears to have a negative effect on Rhizobiales.

Of course, Azospirillales and Rhizobiales are both well known as PGPR. The genus *Azospirillum* consists of 15 species, living in soil, non-pathogenic, plant growth promoting, motile including chemotaxis towards oxygen, and nitrogen fixing (59). *A. brasilense* is a generalist that forms associations with a broad range of plants (60); maize (11),wheat (61), tomatoes (62), cucumbers (*Cucumis sativus*) (63), and strawberries (*Fragaria* x *ananassa*) (64). Members of *Rhizobium* in contrast are much more host specific. The species *Rhizobium leguminosarum* bv. *viciae* as one example is specific for members from the *Fabeae* family; peas (*Pisum sativum*) (65), lentils (*Lens culinaris*) (66), and faba beans (*Vicia faba*) (67). The association of *R. leguminosarum* bv. *viciae* with their host is a true symbiosis resulting in the formation of root nodules and the ability to fix nitrogen (68). We are finding it interesting that inoculating tomatoes with *A. brasilense* Sp7 has a negative effect on Rhizobiales. While members from the Rhizobiales have been found in the tomato rhizosphere before (40), it is possible that *A. brasilense* Sp7 is the better PGPR for tomatoes than any of the Rhizobiales.

As a final observation, *A. brasilense* Sp7 is present in the tomato rhizosphere at low abundances. We failed to detect live bacterial counts of our inoculant. Likewise, we did not receive a signal in the dPCR for *A. brasilense* Sp7 either. 16S rDNA abundances were low throughout all test groups. This confirms previous observations that *Azospirillum* is rarely mentioned in metagenomics studies even when used as inoculant and requires 16S rDNA sequencing for detection (17). We conclude that *A. brasilense* must be effective even at low abundances.

Materials and Methods

Biological materials

Bacteria used for this study were *A. brasilense* Sp7 (69) (also known as DSMZ 1690), kindly provided by Dr. Gladys Alexandre (University of Tennessee, Knoxville, TN) and *P. syringae* pv. tomato DC3000 (ATCC BAA-871) (70). *A. brasilense* Sp7 was cultured in Tryptone Yeast extract (TY: tryptone, 5 g/l; yeast extract, 3 g/l; $CaCl_2 \cdot 6H_2O$, 1.3 g/l (71)). *P. syringae* pv. tomato DC3000 was grown in liquid King's B medium (20 g/l proteose peptone, 1.5 g/l K_2HPO_4, 10 ml/l glycerol, 1.5 g/l $MgSO_4 \cdot 7\ H_2O$), pH 7,2 $\pm$ 0.2) (72), supplemented with 50 µg/ml rifampicin. For plant inoculation, cultures were grown on King's B agar plates (15 g/l agar) at 28°C for 24 to 48 hours. Bacteria were collected from plates and resuspended in 10 mM $MgCl_2$ to the desired colony forming units (CFU)/ml of culture.

Yellow pear tomato seeds (SKU34924) were from True Leaf Market (Salt Lake City, UT). Seeds were surface-sterilized for 30 s in 95% ethanol and 5 min in 2% bleach, then rinsed 10 times with sterile dH_2O. Seeds germinated for 3 days on 0.8% agar in sterile dH_2O. For experiments with seedling exudate, tomato exudate was produced from 1 g of freshly germinated seeds in 10 ml of dH_2O as previously described (22). Seeds were germinated under three separate conditions: sterile dH_2O, seedling exudate, or cytidine. Seedling exudate was supplemented to the water agar at a concentration of 1.5 mg of exudate dry weight/ml dH_2O. Cytidine was supplemented at a concentration of 100 mM. Germinated seeds were planted when approximately half an inch of root was visible.

Plant growth

Tomato growth medium was a sterilized mix of soil (Promix BX General Purpose, 10280; Premier Horticulture Inc. Canada, Québec, Canada) and vermiculite (Vermiculite

Medium PVP; PVP Industries, North Bloomfield, OH) at a ratio of 1:1 (w/w). Germinated seeds were planted into the center of pots of ~4 inch in diameter and 6 inch in height; pots had been sprayed with ethanol the day before planting, sterile cotton balls were used to cover the holes. *A. brasilense* Sp7 was inoculated at approximately 10^3 to 10^4 CFU in 1 ml of H_2O to the location of the germinated seed at the time of planting. Plants were grown at the Jack Dalrymple Agricultural Research Complex at NDSU in a Gen 2000 growth chamber (Conviron, Pembina, ND) at 26°C. In both cases, light was for 16 hours. For one week experiments, plants were not fertilized. For longer experiments, we used TomatoMaker^{TM} from Baker Garden (Fargo, ND) according to the manufacturer's instructions.

Phytopathogen experiment

Tomato seedlings germinated in sterile dH_2O, exudate, or cytidine were planted and inoculated with/without *A. brasilense* Sp7 to the location of the planted seed at the time of planting. Four weeks old tomato plants were dip-inoculated with *P. syringae* pv. tomato DC3000 following the protocol by Chakravarty *et al.* (23). Briefly, the plants were bagged for 24 h to create a high-humidity environment. Plants were dipped for 30 s in 3 x 10^7 CFU ml^{-1} in 10 mM $MgCl_2$. Plants were air dried and incubated in a Gen 2000 growth chamber at 26°C with 80% relative humidity and 16 h of light. Five to seven days after the phytopathogen challenge, plants were photographed and assessed for disease symptoms.

Disease data were collected from 3 to 6 plants per test group in 3 to 4 replicate experiments for a total of 18 plants. Disease symptoms started with dark necrotic lesions on the leaves, then wilting of the leaves. In severe cases, this was followed by leaf and ultimately plant death. We expressed disease symptoms as percent death of the leaves from each plant. One completely healthy plant that had not been challenged with the pathogen and one severely

diseased plant were used as comparison for the assessment of percent death of each of the plants. The assessment was done by at least two researchers in steps of 10%. Examples of plants that were assessed as 0% dead, 50% dead, and 90% dead are presented in Supplemental Figure 1.

For live bacterial counts, we used 3 to 6 plants per test group in 2 to 3 replicate phytopathogen experiments to a maximum of 14 plants. Live bacterial counts were obtained from homogenates that were produced from 6 leaf discs per plant that were punched with a 1/4 inch sterile cork borer. Weighed leaf discs were homogenized in 10 mM $MgCl_2$, using sterile pestles. The homogenates were serially diluted and plated onto King's B agar plates to determine counts of species from the *Pseudomonas* genus (72). Bacterial counts were expressed as CFU/g of plant material.

For disease symptoms and *Pseudomonas* counts, data are presented as Box and Whisker plots generated with GraphPad Prism. Statistical analysis was done by one-way ANOVA, followed with Tukey for pairwise comparisons between test groups. A *p*-value below 0.05 was indicative of a statistically significant difference between two test groups.

16S rDNA analysis

For the determination of 16S rDNA abundances on leaves, DNA was isolated from leaf homogenates from three plants from one phytopathogen experiment. For the determination of 16S rDNA abundances on roots, roots from three plants from one phytopathogen experiment were washed with H_2O thoroughly but carefully, so that most of the soil would be gone, but the outside of the roots would still be intact. This sampling would give us the epiphytic and endophytic microbiome of leaves and roots.

Homogenates were produced from approximately 50 mg of plant material by using the Cole-Parmer HG-200 GenoLyteR Compact Homogenizer (Cole-Parmer, Vernon Hills, IL) at

2,000 rpm for 1 min. DNA extraction was done with the Qiagen Plant Pro kit (Qiagen, Hilden, Germany). Quality of the DNA samples was analyzed with the Nanodrop One Spectrophotometer, quantity with the Qubit 4 Fluorometer (Fisher Scientific, Hampton, NH). Samples were diluted to 1 ng/µl. The construction of the library and 16S rDNA sequencing were done at the Dr. Thomas Glass Biotech Innovation Core at NDSU. We used the QIAseq 16S/ITS Region Panel (Qiagen) for the generation of the 16S rDNA library. The primers used were 341f:CCTACGGGNGGCWGCAG and 785r:GACTACHVGGGTATCTAATCC, which amplify the V3/V4 hyper variable region of the 16S rDNA (Qiagen). We followed the PCR protocol from the manufacturer and cleaned the resulting PCR products with QIAseq bead cleanup. The index PCR reaction was done with unique dual indexes for each sample, PCR products were cleaned with QIAseq bead cleanup. Samples were quantified with the Qubit 4 Fluorometer and analyzed with the 4200 Tape Station (Agilent, Santa Clara, CA). Sequencing was performed using the P1 XLEAP-SBS 600 cycle sequencing kit on the NextSeq 1000 (Illumina, San Diego, CA).

Phyllosphere and rhizosphere data were analyzed separately. Fastq files were imported into CLC Genomics Workbench (Qiagen) for analysis using the Microbial Genomics Module. The Data QC and OTU clustering workflow was used to trim adaptors, poly G regions, ambiguities and sequences not meeting the quality threshold of 0.05. Reference based OTU clustering using the Silva SSU 99% (138.2) database was performed using the similarity percent specified by the database. Minimum occurrence was set at 2. The species identifiers or taxonomies in the CLC Workbench are from the Earth Microbiome Project (https://earthmicrobiome.org/). The resulting abundance tables were exported to Excel separately for phyllosphere and rhizosphere and further analyzed. These two tables are provided as online supplements and include the ASU (Supplemental Tables 1 and 2).

Step 1 of the analysis was to identify our inoculant *A. brasilense* Sp7 and our challenge *P. syringae* pv. tomato among the bacterial species that the CLC Workbench bioinformatics analysis had associated with the ASUs according to the Earth Microbiome Project. This was done experimentally. We grew liquid cultures of each strain and included the data in separate columns of Supplemental Table 2; *A. brasilense* Sp7 (column BG) and *P. syringae* pv. tomato DC3000 (column BH). Each of these columns show one single large abundance in the 6 digit range. For our inoculant, this large abundance was *A. brasilense* AF533354.1.1439. Our challenge strain was *P. amygdali* pv. morsprunorum AB0011445.1.1538, incorrectly designated by the CLC Workbench bioinformatics analysis. For additional confirmation, ASU from those two species were subjected to a BLAST analysis (https://blast.ncbi.nlm.nih.gov/Blast.cgi). These data are included in Supplemental Table 3 and serve as additional confirmation that *P. amygdali* pv. morsprunorum is indeed our phytopathogen *P. syringae* pv. tomato DC3000. Note that Supplemental Table 3 contains a small number of other taxonomies that we checked with BLAST and changed accordingly.

Step 2 was to filter out small abundances that added a lot of taxonomies to the data set but not a lot of information. In Supplemental Table 1, we filtered out all DNA abundances (rows) from organisms that had combined abundances $\leq$49 added across all test groups and replicates (36 columns). We also removed plant and fungal taxonomies and limited the data set to microbial species. One tab of plant taxonomies was retained for tomato data. In Supplemental Table 2, we filtered out abundances from organisms that had combined abundances $\leq$499 and removed plant and fungal taxonomies. On separate tabs, we split the data set up into non Proteobacteria, Alphaproteobacteria, and Beta/Gammaproteobacteria.

Step 3 was the analysis of 16S rDNA abundances from our challenge pathogen *P. syringae* pv. tomato DC3000 in the phyllosphere and our inoculant *A. brasilense* Sp7 in the rhizosphere. In Supplemental Table 1, we used the single row of *P. syringae* DC3000 data and the 15 rows of tomato data. The two data sets were statistically analyzed with separate one-way ANOVAs to compare all 12 test groups. For the *P. syringae* DC3000 data, a second ANOVA was performed across the 6 test groups of plants challenged with *P. syringae* pv. tomato DC3000 (+Ps). In Supplemental Table 2, we used the sole row of *A. bra*. data. Data from both analyses are presented as bar plots in GraphPad Prism, including the mean across the three replicate experiments and the standard deviation. Note that inoculant and challenge strains were removed from all other analyses.

Step 4 was the generation of phylogenetic trees. For the phyllosphere, we used the data from Supplemental Table 1 in the >50 tab, these are 67 taxonomies represented in any of the 12 test groups with an abundance summed across all test groups of 50 or more. These data were converted into a FASTA file and loaded into Galaxy (usegalaxy.eu/). We performed a multiple sequence alignment with MAFFT, followed by FASTTREE. The Newick file (.nhx) from the maximum likelihood computation was used in iTOL (itol.embl.de). Using the mid-point root, the circular tree was selected for presentation. Note that the taxonomies were abbreviated as part of the production of the FASTA file. Abbreviations are included in Supplemental Table 1 as a separate column on the >50 tab. As a final step, a color strip was produced that coded the bacterial orders with different colors. This was uploaded into iTOL as a txt file. For the rhizosphere, we used the data from Supplemental Table 2 in the non proteos tab to generate the FASTA file and produce the phylogenetic tree in a way that was identical to phyllosphere. The

color strip file coded the phyla with different colors. The large number of Proteobacteria were not graphed in the phylogenetic tree.

Step 5 was the analysis of 16S rDNA abundances within phyllosphere and rhizosphere. First, alpha diversity was calculated as Shannon's index from relative abundances of the 67 or 280 taxonomies from phyllosphere and rhizosphere. This was done for each replicate in Excel with the following function: (COUNTIF(AI2:AI70, ">1"). Data were transferred into GraphPad Prism and graphed as floating bars. Second, relative abundances were summed over the 67 or 280 taxonomies from phyllosphere and rhizosphere. This was done separately for each of the three replicates in Excel, data were transferred into GraphPad Prism and graphed as floating bars. Third, for the generation of the heatmaps, 16S rDNA abundances from taxonomies that represent the different bacterial orders were summed across all species from the respective order in designated tabs of Supplemental Tables 1 and 2. Mean percent abundances across the three replicates were used and visualized in GraphPad Prism. Note that for the phyllosphere, only test groups that were challenged with the pathogen were included in the heatmap. For the rhizosphere, all 12 test groups were included. Fourth, the same data set was used for principal component analysis (PCA) in GraphPad Prism. The PC scores (treatments) and Biplot analysis (treatment and bacterial orders) were graphed. We computed association strength between treatments and bacterial orders with cosinus similarity, a metric that quantifies how similar two non-zero vectors are by calculating the cosine of the angle between them. This was done with the following Python code:

```
order = np.array([PC1, PC2])
treatment = np.array([PC1, PC2])
cosine_similarity = np.dot(order, treatment) / (np.linalg.norm(order) *
np.linalg.norm(treatment))
print("Cosine similarity:", cosine_similarity)
```

Digital PCR

From the same DNA samples that were used for 16S rDNA sequencing, we performed digital PCR to confirm 16S rDNA data for our challenge pathogen *P. syringae* pv. tomato DC3000. Primers for *P. syringae* pv. tomato DC3000 were PST-hrpL_e_fwd, 5'-TTTCAACATGCCAGCAAACC-3' and PST-hrpL_e_rev, 5'-GATGCCCCTCTACCTGATGA-3' as described (29). The probe was PST-hrpL_TP, 5'- GCTGAACCTGATCCGCAATCAC-3', marked with the yellow fluorescence dye HEX.

Each PCR reaction mix of 40 µl contained between 50 and 200 ng of DNA, 1 x PCR mix, 0.8 µM primer mix, 0.4 µM probe, and 0.25 U EcoRI in RNAse free water. The PCR reactions were performed in a QIAcuity Digital PCR System (Qiagen) on 24 well QIAcuity Nanoplates at 40 cycles of annealing/extension at 55°C for 30 s and denaturation at 95°C for 15 s. After 40 cycles, fluorescence was measured in each of the 25,000 partitions of a well. Individual reactions were considered positive when a threshold of 50 to 150 was achieved. The original data were expressed as count of positive and negative reactions in the partitions and computed to copies/µl in the QIAcuity Software Suite v2.1.7.182. Given the start concentration of DNA, these data were converted to copies/ng of DNA. Data were graphed as floating bars in GraphPad Prism, statistical analysis was done with ANOVA.

Acknowledgements

The authors thank Dr. Gladys Alexandre (University of Tennessee, Knoxville, TN) for providing the *A. brasilense* Sp7 strain and Dr. Melania Filiatrault (USDA/ARA, Ithaca, NY) for many helpful discussions. We thank Scott Hoselton and Kaycie Schmidt from the Dr. Thomas Glass Biotech Innovation Core at NDSU for performing the 16S rDNA analysis and helping us with the dPCR. The research was funded by Specialty Crop Block Grant 22-242 from the

USDA/NIFA and grant 24-2030 from the North Dakota Agricultural Products and Utilization Commission. BMP was supported, in part, by the intramural research program of the U.S. Department of Agriculture, National Institute of Food and Agriculture, Hatch project accession number, 7009493. The findings and conclusions in this preliminary publication have not been formally disseminated by the U. S. Department of Agriculture and should not be construed to represent any agency determination or policy.

Figure Legends

Fig. 1. Disease symptoms. For the disease assessments, we collected percent leaf death data from up to six plants per test group in 3 to 4 replicate experiments for a maximum of 18 plants. The blunt end lines across all test groups indicate the *p*-values from the one-way ANOVA. The open ended lines between two bars are the *p*-values from the pairwise comparisons with Tukey. ns, *p*-value >0.05; *, *p*-value 0.01 - 0.05; **, *p*-value 0.001 – 0.01; ***, *p*-value <0.001; **** *p*-value < 0.0001.

Fig. 2. Live bacterial counts on tomato leaves. For live bacterial counts, we determined $\log_{10}$ CFU/g plant material from 3 to 6 plants per test group in 2 to 3 replicate experiments to a maximum of 14 plants. The blunt end line across all test groups indicates the *p*-value from the one-way ANOVA. The open ended lines between two bars are the *p*-values from the pairwise comparisons with Tukey. ns, *p*-value >0.05; *, *p*-value 0.01 - 0.05; **, *p*-value 0.001 – 0.01; ***, *p*-value <0.001; **** *p*-value < 0.0001.

Fig. 3. DNA analysis for *P. syringae* pv. tomato DC3000 and tomato 16S rDNA was sequenced from leaf homogenates from 3 plants from one phytopathogen experiment (Panel A). Copies of the *hrpL* gene were determined from the same leaf homogenates by dPCR (Panel B). The blunt end lines across all test groups for the *P. syringae* and the tomato analyses indicate the *p*-values from the one-way ANOVA.

Fig. 4. 16S rDNA abundances for *A. brasilense* Sp7. 16S rDNA was analyzed from root homogenates from 3 plants from one phytopathogen experiment. The blunt end line across all test groups indicates the *p*-value from the one-way ANOVA. The open end line between two bars indicates the *p*-value from the pairwise comparison with Tukey. ns, *p*-value >0.05; *, *p*-value 0.01 - 0.05; **, *p*-value 0.001 – 0.01; ***, *p*-value <0.001; **** *p*-value < 0.0001.

Fig. 5. Phylogenetic tree from the tomato phyllosphere. 16S rDNA was analyzed from leaf homogenates from 3 plants from one of the replicate phytopathogen experiments. The phylogenetic tree was generated in Galaxy and visualized in iTOL from the 67 bacterial species that exhibited 16S rDNA abundances higher than 50 across all test groups and replicates.

Fig. 6. Bacterial diversity and abundances within the tomato phyllosphere. Fig. 6A demonstrates alpha diversity as Shannon index, Fig. 6B the sum abundances across all bacterial species per test group. Fig. 6C is the heat map for percent 16rDNA abundances from all bacterial species within each bacterial order in each of the six test groups that were challenged with the pathogen. PCA analysis is presented as PC scores in Fig. 6D and Biplot in Fig. 6E.

Fig. 7. Phylogenetic tree from the tomato rhizosphere. 16S rDNA was analyzed from root homogenates from 3 plants from one of the replicate phytopathogen experiments. The phylogenetic tree was generated in Galaxy and visualized in iTOL from the 102 bacterial species that exhibited 16S rDNA abundances higher than 500 across all test groups and replicates and were not from the phylum Proteobacteria.

Fig. 8. Bacterial diversity and abundances within the tomato rhizosphere. Fig. 8A demonstrates alpha diversity as Shannon index, Fig. 8B the sum abundances across all bacterial species per test group. Fig. 8C is the heat map for percent 16rDNA abundances from all bacterial species within each bacterial order.

Fig. 9. PCA analysis. Fig. 19A shows the PC scores and Fig. 9B the Biplot.

Fig. 10. 16S rDNA abundances for Azospirillales and Rhizobiales. The open lines between two test groups indicate the *p*-values from the Tukey *post hoc* test.

References

1. Preston GM. 2000. *Pseudomonas syringae* pv. tomato: the right pathogen, of the right plant, at the right time. Mol Plant Pathol 1:263-75.
2. Bergougnoux V. 2014. The history of tomato: from domestication to biopharming. Biotechnol Adv 32:170-89.
3. Ma LJ, Geiser DM, Proctor RH, Rooney AP, O'Donnell K, Trail F, Gardiner DM, Manners JM, Kazan K. 2013. *Fusarium* pathogenomics. Annu Rev Microbiol 67:399-416.
4. El-Fatah B, Imran M, Abo-Elyousr KAM, Mahmoud AF. 2023. Isolation of *Pseudomonas syringae* pv. tomato strains causing bacterial speck disease of tomato and marker-based monitoring for their virulence. Mol Biol Rep 50:4917-4930.
5. Whalen MC, Innes RW, Bent AF, Staskawicz BJ. 1991. Identification of *Pseudomonas syringae* pathogens of *Arabidopsis* and a bacterial locus determining avirulence on both *Arabidopsis* and soybean. Plant Cell 3:49-59.
6. Santamaría-Hernando S, López-Maroto Á, Galvez-Roldán C, Munar-Palmer M, Monteagudo-Cascales E, Rodríguez-Herva JJ, Krell T, López-Solanilla E. 2022. *Pseudomonas syringae* pv. tomato infection of tomato plants is mediated by GABA and l-Pro chemoperception. Mol Plant Pathol 23:1433-1445.
7. Cerna-Vargas JP, Santamaría-Hernando S, Matilla MA, Rodríguez-Herva JJ, Daddaoua A, Rodríguez-Palenzuela P, Krell T, López-Solanilla E. 2019. Chemoperception of specific amino acids controls phytopathogenicity in *Pseudomonas syringae* pv. tomato. mBio 10.
8. Xin XF, He SY. 2013. *Pseudomonas syringae* pv. tomato DC3000: a model pathogen for probing disease susceptibility and hormone signaling in plants. Annu Rev Phytopathol 51:473-98.
9. Elsharkawy MM, Khedr AA, Mehiar F, El-Kady EM, Alwutayd KM, Behiry SI. 2023. Rhizobacterial colonization and management of bacterial speck pathogen in tomato by *Pseudomonas* spp. Microorganisms 11.
10. Pereg-Gerk L, Paquelin A, Gounon P, Kennedy IR, Elmerich C. 1998. A transcriptional regulator of the LuxR-UhpA family, FlcA, controls flocculation and wheat root surface colonization by *Azospirillum brasilense* Sp7. Mol Plant Microbe Interact 11:177-87.
11. Vidotti MS, Matias FI, Alves FC, Pérez-Rodríguez P, Beltran GA, Burgueño J, Crossa J, Fritsche-Neto R. 2019. Maize responsiveness to *Azospirillum brasilense*: Insights into genetic control, heterosis and genomic prediction. PLoS One 14:e0217571.
12. Pellegrini M, Ercole C, Di Zio C, Matteucci F, Pace L, Del Gallo M. 2020. *In vitro* and *in planta* antagonistic effects of plant growth-promoting rhizobacteria consortium against soilborne plant pathogens of *Solanum tuberosum* and *Solanum lycopersicum*. FEMS Microbiol Lett 367.
13. Correa OS, Romero AM, Montecchia MS, Soria MA. 2007. Tomato genotype and *Azospirillum* inoculation modulate the changes in bacterial communities associated with roots and leaves. J Appl Microbiol 102:781-6.
14. da Cunha ET, Pedrolo AM, Paludo F, Scariot MC, Arisi ACM. 2020. *Azospirillum brasilense* viable cells enumeration using propidium monoazide-quantitative PCR. Arch Microbiol 202:1653-1662.

15. Botta AL, Santacecilia A, Ercole C, Cacchio P, Del Gallo M. 2013. *In vitro* and *in vivo* inoculation of four endophytic bacteria on *Lycopersicon esculentum*. N Biotechnol 30:666-74.
16. Bashan Y, De-Bashan LE. 2002. Protection of tomato seedlings against infection by *Pseudomonas syringae* pv. tomato by using the plant growth-promoting bacterium *Azospirillum brasilense*. Appl Environ Microbiol 68:2637-43.
17. Nievas S, Coniglio A, Takahashi WY, López GA, Larama G, Torres D, Rosas S, Etto RM, Galvão CW, Mora V, Cassán F. 2023. Unraveling *Azospirillum*'s colonization ability through microbiological and molecular evidence. J Appl Microbiol 134.
18. Ganusova EE, Rost M, Aksenova A, Abdulhussein M, Holden A, Alexandre G. 2023. *Azospirillum brasilense* AerC and Tlp4b cytoplasmic chemoreceptors are promiscuous and interact with the two membrane-bound chemotaxis signaling clusters mediating chemotaxis responses. J Bacteriol 205:e0048422.
19. Ganusova EE, Russell MH, Patel S, Seats T, Alexandre G. 2024. An *Azospirillum brasilense* chemoreceptor that mediates nitrate chemotaxis has conditional roles in the colonization of plant roots. Appl Environ Microbiol 90:e0076024.
20. Ganusova EE, Vo LT, Abraham PE, O'Neal Yoder L, Hettich RL, Alexandre G. 2021. The *Azospirillum brasilense* core chemotaxis proteins CheA1 and CheA4 link chemotaxis signaling with nitrogen metabolism. mSystems 6.
21. Alexandre G, Greer SE, Zhulin IB. 2000. Energy taxis is the dominant behavior in *Azospirillum brasilense*. J Bacteriol 182:6042-6048.
22. Nisha FA, Tagoe JNA, Pease AB, Horne SM, Ugrinov A, Geddes BA, Prüß BM. 2024. Plant seedlings of peas, tomatoes, and cucumbers exude compounds that are needed for growth and chemoattraction of *Rhizobium leguminosarum* bv. *viciae* 3841 and *Azospirillum brasilense* Sp7. Can J Microbiol 70:150-162.
23. Chakravarthy S, Butcher BG, Liu Y, D'Amico K, Coster M, Filiatrault MJ. 2017. Virulence of *Pseudomonas syringae* pv. tomato DC3000 Is influenced by the catabolite repression control protein Crc. Mol Plant Microbe Interact 30:283-294.
24. Wei HL, Collmer A. 2018. Defining essential processes in plant pathogenesis with *Pseudomonas syringae* pv. tomato DC3000 disarmed polymutants and a subset of key type III effectors. Mol Plant Pathol 19:1779-1794.
25. Lindeberg M, Biehl BS, Glasner JD, Perna NT, Collmer A, Collmer CW. 2009. Gene Ontology annotation highlights shared and divergent pathogenic strategies of type III effector proteins deployed by the plant pathogen *Pseudomonas syringae* pv tomato DC3000 and animal pathogenic *Escherichia coli* strains. BMC Microbiol 9 Suppl 1:S4.
26. Janda M, Rybak K, Krassini L, Meng C, Feitosa-Junior O, Stigliano E, Szulc B, Sklenar J, Menke FLH, Malone JG, Brachmann A, Klingl A, Ludwig C, Robatzek S. 2023. Biophysical and proteomic analyses of *Pseudomonas syringae* pv. tomato DC3000 extracellular vesicles suggest adaptive functions during plant infection. mBio 14:e0358922.
27. Namgung M, Lim YJ, Kang MK, Oh CS, Park DH. 2019. *Pseudomonas syringae* pv. tomato DC3000 improves *Escherichia coli* O157:H7 survival in tomato plants. J Microbiol Biotechnol 29:1975-1981.
28. Djami-Tchatchou AT, Li ZA, Stodghill P, Filiatrault MJ, Kunkel BN. 2022. Identification of Indole-3-Acetic Acid-regulated genes in *Pseudomonas syringae* pv. tomato strain DC3000. J Bacteriol 204:e0038021.

29. Peňázová E, Dvořák M, Ragasová L, Kiss T, Pečenka J, Čechová J, Eichmeier A. 2020. Multiplex real-time PCR for the detection of *Clavibacter michiganensis* subsp. *michiganensis*, *Pseudomonas syringae* pv. tomato and pathogenic *Xanthomonas* species on tomato plants. PLoS One 15:e0227559.
30. Johnsen K, Nielsen P. 1999. Diversity of *Pseudomonas* strains isolated with King's B and Gould's S1 agar determined by repetitive extragenic palindromic-polymerase chain reaction, 16S rDNA sequencing and Fourier transform infrared spectroscopy characterisation. FEMS Microbiol Lett 173:155-162.
31. Reddy Priya P, Selastin Antony R, Gopalaswamy G, Balachandar D. 2016. Development of sequence-characterized amplified region (SCAR) markers as a quality standard of inoculants based on *Azospirillum*. Arch Microbiol 198:257-67.
32. Yin J, Zhang Z, Zhu C, Wang T, Wang R, Ruan L. 2022. Heritability of tomato rhizobacteria resistant to Ralstonia solanacearum. Microbiome 10:227.
33. Huang J, Zhu L, Lu X, Cui F, Wang J, Zhou C. 2023. A simplified synthetic rhizosphere bacterial community steers plant oxylipin pathways for preventing foliar phytopathogens. Plant Physiol Biochem 202:107941.
34. Ma S, Chen Q, Zheng Y, Ren T, He R, Cheng L, Zou P, Jing C, Zhang C, Li Y. 2025. A tale for two roles: root-secreted methyl ferulate inhibits *P. nicotianae* and enriches the rhizosphere *Bacillus* against black shank disease in tobacco. Microbiome 13:33.
35. Baatsen J, Hosaka GK, Mondin M, Azevedo JL, Hungria M, Quecine MC. 2025. Benzoxazinoids stimulate chemotaxis and act as a signaling molecule in *Azospirillum brasilense* Ab-V5, while showing minor effects on *Pseudomonas protegens* Pf-5. mBio 16:e01414-25.
36. Dong C-JW, L.-L.; Li, Q.; Shang, Q.-M. 2019. Bacterial communities in the rhizosphere, phyllosphere, and endosphere of tomato plant. PLoS One 8:e0223847.
37. Romero FM, Marina M, Pieckenstain FL. 2014. The communities of tomato (*Solanum lycopersicum* L.) leaf endophytic bacteria, analyzed by 16S-ribosomal RNA gene pyrosequencing. FEMS Microbiol Lett 351:187-94.
38. Fagnano FM, Ventorino V, Pasolli E, Romano I, Ambrosino P, Pepe O. 2025. From microbiome to biostimulants: unlocking the potential of tomato root endophytes. BMC Plant Biol 25:427.
39. Lee SM, Kong HG, Song GC, Ryu CM. 2021. Disruption of Firmicutes and Actinobacteria abundance in tomato rhizosphere causes the incidence of bacterial wilt disease. Isme j 15:330-347.
40. Cheng Z, Lei S, Li Y, Huang W, Ma R, Xiong J, Zhang T, Jin L, Haq HU, Xu X, Tian B. 2020. Revealing the variation and stability of bacterial communities in tomato rhizosphere microbiota. Microorganisms 8.
41. Takamatsu K, Toyofuku M, Okutani F, Yamazaki S, Nakayasu M, Aoki Y, Kobayashi M, Ifuku K, Yazaki K, Sugiyama A. 2023. α-Tomatine gradient across artificial roots recreates the recruitment of tomato root-associated Sphingobium. Plant Direct 7:e550.
42. Gao R, Dong H, Liu Y, Yao Q, Li H, Zhu H. 2023. Sphingomonas lycopersici sp. nov., isolated from tomato rhizosphere soil. Int J Syst Evol Microbiol 73.
43. Nakayasu M, Takamatsu K, Kanai K, Masuda S, Yamazaki S, Aoki Y, Shibata A, Suda W, Shirasu K, Yazaki K, Sugiyama A. 2023. Tomato root-associated Sphingobium harbors genes for catabolizing toxic steroidal glycoalkaloids. mBio 14:e0059923.

44. Nakayasu M, Takamatsu K, Yazaki K, Sugiyama A. 2022. Plant specialized metabolites in the rhizosphere of tomatoes: secretion and effects on microorganisms. Biosci, Biotech, Biochem 87:13-20.
45. Nakayasu M, Ohno K, Takamatsu K, Aoki Y, Yamazaki S, Takase H, Shoji T, Yazaki K, Sugiyama A. 2021. Tomato roots secrete tomatine to modulate the bacterial assemblage of the rhizosphere. Plant Physiol 186:270-284.
46. Zhou X, Zhang J, Khashi URM, Gao D, Wei Z, Wu F, Dini-Andreote F. 2023. Interspecific plant interaction via root exudates structures the disease suppressiveness of rhizosphere microbiomes. Mol Plant 16:849-864.
47. Korenblum E, Dong Y, Szymanski J, Panda S, Jozwiak A, Massalha H, Meir S, Rogachev I, Aharoni A. 2020. Rhizosphere microbiome mediates systemic root metabolite exudation by root-to-root signaling. Proc Natl Acad Sci U S A 117:3874-3883.
48. Wen T, Xie P, Liu H, Liu T, Zhao M, Yang S, Niu G, Hale L, Singh BK, Kowalchuk GA, Shen Q, Yuan J. 2023. Tapping the rhizosphere metabolites for the prebiotic control of soil-borne bacterial wilt disease. Nat Commun 14:4497.
49. Feng Z, Liang Q, Yao Q, Bai Y, Zhu H. 2024. The role of the rhizobiome recruited by root exudates in plant disease resistance: current status and future directions. Environ Microbiome 19:91.
50. Zheng Y, Cao X, Zhou Y, Ma S, Wang Y, Li Z, Zhao D, Yang Y, Zhang H, Meng C, Xie Z, Sui X, Xu K, Li Y, Zhang CS. 2024. Purines enrich root-associated *Pseudomonas* and improve wild soybean growth under salt stress. Nat Commun 15:3520.
51. Yang K, Fu R, Feng H, Jiang G, Finkel O, Sun T, Liu M, Huang B, Li S, Wang X, Yang T, Wang Y, Wang S, Xu Y, Shen Q, Friman VP, Jousset A, Wei Z. 2023. RIN enhances plant disease resistance via root exudate-mediated assembly of disease-suppressive rhizosphere microbiota. Mol Plant 16:1379-1395.
52. Marin VR, Ferrarezi JH, Vieira G, Sass DC. 2019. Recent advances in the biocontrol of Xanthomonas spp. World J Microbiol Biotechnol 35:72.
53. Sultana F, Hossain MM. 2022. Assessing the potentials of bacterial antagonists for plant growth promotion, nutrient acquisition, and biological control of Southern blight disease in tomato. PLoS One 17:e0267253.
54. Brooke JS. 2012. *Stenotrophomonas maltophilia*: an emerging global opportunistic pathogen. Clin Microbiol Rev 25:2-41.
55. Jin Y, Wu X, Sa R, Dong H, Xiong Y, He S, Li C, Geng X. 2022. First report of *Enterobacter cloacae* causing stem, leaf and fruit rot on tomato in China. Plant Dis doi:10.1094/pdis-08-22-1749-pdn.
56. Stokes W, Peirano G, Matsumara Y, Nobrega D, Pitout JDD. 2022. Population-based surveillance of *Enterobacter cloacae* complex causing blood stream infections in a centralized Canadian region. Eur J Clin Microbiol Infect Dis 41:119-125.
57. Berg G, Eberl L, Hartmann A. 2005. The rhizosphere as a reservoir for opportunistic human pathogenic bacteria. Environmental Microbiology 7:1673-1685.
58. Kim JS, Yoon SJ, Park YJ, Kim SY, Ryu CM. 2020. Crossing the kingdom border: Human diseases caused by plant pathogens. Environ Microbiol 22:2485-2495.
59. Alexandre G. 2017. *Azospirillum brasilense*, a beneficial soil bacterium: isolation and cultivation. Curr Protoc Microbiol 47:3e.1.1-3e.1.10.

60. Tarrand JJ, Krieg NR, Döbereiner J. 1978. A taxonomic study of the *Spirillum lipoferum* group, with descriptions of a new genus, *Azospirillum* gen. nov. and two species, *Azospirillum lipoferum* (Beijerinck) comb. nov. and *Azospirillum brasilense* sp. nov. Can J Microbiol 24:967-80.
61. Vazquez A, Zawoznik M, Benavides MP, Groppa MD. 2021. *Azospirillum brasilense* Az39 restricts cadmium entrance into wheat plants and mitigates cadmium stress. Plant Sci 312:111056.
62. El-Beltagi HS, Ahmad I, Basit A, Abd El-Lateef HM, Yasir M, Tanveer Shah S, Ullah I, Elsayed Mohamed Mohamed M, Ali I, Ali F, Ali S, Aziz I, Kandeel M, Zohaib Ikram M. 2022. Effect of *Azospirillum* and *Azotobacter* species on the performance of cherry tomato under different salinity levels. Gesunde Pflanzen 74:487-499.
63. Marastoni L, Pii Y, Maver M, Valentinuzzi F, Cesco S, Mimmo T. 2019. Role of *Azospirillum brasilense* in triggering different Fe chelate reductase enzymes in cucumber plants subjected to both nutrient deficiency and toxicity. Plant Physiol Biochem 136:118-126.
64. Pedraza RO, Motok J, Salazar SM, Ragout AL, Mentel MI, Tortora ML, Guerrero-Molina MF, Winik BC, Díaz-Ricci JC. 2010. Growth-promotion of strawberry plants inoculated with *Azospirillum brasilense*. World J Microbiol Biotechnol 26:265-272.
65. Vanderlinde EMM, A.; Harrison, J.J.; Koval, S.F.; Foreman, D.L.; Ceri, H.; Kannenberg, E.L.; Carlson, R.W.; Yost, C.K. 2009. *Rhizobium leguminosarum* biovar *viciae* 3841, deficient in 27-hydroxyoctasanoate-modified lipopolysaccharide, is impaired in desiccation tolerance, biofilm formation, and motility. Microbiology 155:3055-3069.
66. Sijilmassi B, Filali-Maltouf A, Boulahyaoui H, Kricha A, Boubekri K, Udupa S, Kumar S, Amri A. 2020. Assessment of genetic diversity and symbiotic efficiency of selected *Rhizobia* strains nodulating lentil (*Lens culinaris* Medik.). Plants (Basel) 10.
67. Boivin S, Mahé F, Debellé F, Pervent M, Tancelin M, Tauzin M, Wielbo J, Mazurier S, Young P, Lepetit M. 2021. Genetic variation in host-specific competitiveness of the symbiont *Rhizobium leguminosarum* symbiovar *viciae*. Front Plant Sci 12:719987.
68. Jiménez-Guerrero I, Acosta-Jurado S, Del Cerro P, Navarro-Gómez P, López-Baena FJ, Ollero FJ, Vinardell JM, Pérez-Montaño F. 2017. Transcriptomic studies of the effect of *nod* gene-inducing molecules in *Rhizobia*: different weapons, one purpose. Genes (Basel) 9:1.
69. Eskew DF, D.D. 1977. Nitrogen fixation, denitrification, and pleomorphic growth in a highly pigmented *Spirillum lipoferum.* Appl Environ Microbiol 34:582-585.
70. Buell CR, Joardar V, Lindeberg M, Selengut J, Paulsen IT, Gwinn ML, Dodson RJ, Deboy RT, Durkin AS, Kolonay JF, Madupu R, Daugherty S, Brinkac L, Beanan MJ, Haft DH, Nelson WC, Davidsen T, Zafar N, Zhou L, Liu J, Yuan Q, Khouri H, Fedorova N, Tran B, Russell D, Berry K, Utterback T, Van Aken SE, Feldblyum TV, D'Ascenzo M, Deng WL, Ramos AR, Alfano JR, Cartinhour S, Chatterjee AK, Delaney TP, Lazarowitz SG, Martin GB, Schneider DJ, Tang X, Bender CL, White O, Fraser CM, Collmer A. 2003. The complete genome sequence of the *Arabidopsis* and tomato pathogen *Pseudomonas syringae* pv. tomato DC3000. Proc Natl Acad Sci U S A 100:10181-6.
71. Beringer JE. 1974. R factor transfer in *Rhizobium leguminosarum*. Microbiology 84:188-198.

72. King EO, Ward MK, Raney DE. 1954. Two simple media for the demonstration of pyocyanin and fluorescin. J Lab Clin Med 44:301-7.

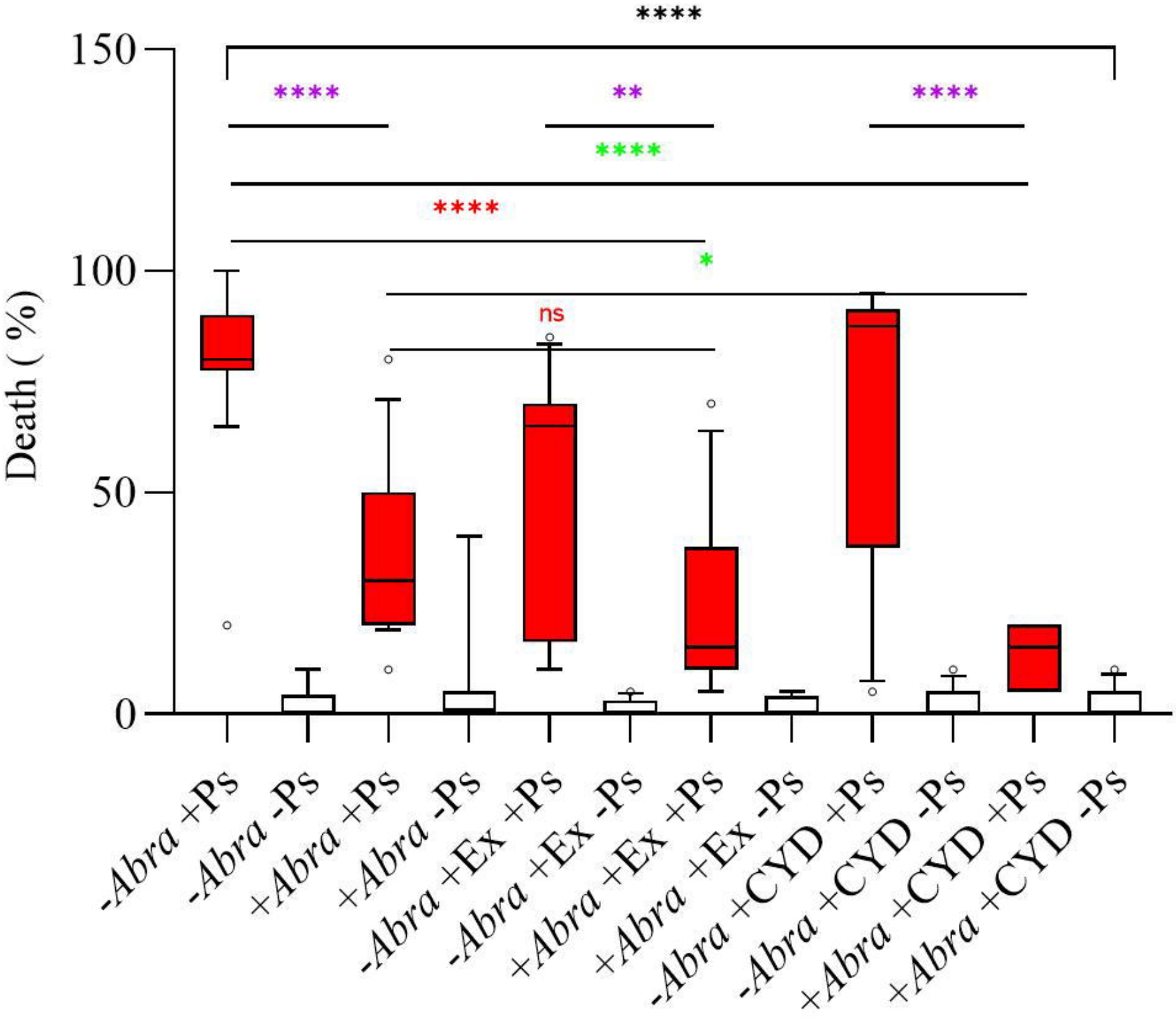
****
150
100
50
0
Death (%)
****
**
****
****
****
*
ns
-Abra +Ps
-Abra -Ps
+Abra +Ps
+Abra -Ps
-Abra +Ex +Ps
-Abra +Ex -Ps
+Abra +Ex +Ps
+Abra +Ex -Ps
-Abra +CYD +Ps
-Abra +CYD -Ps
+Abra +CYD +Ps
+Abra +CYD -Ps

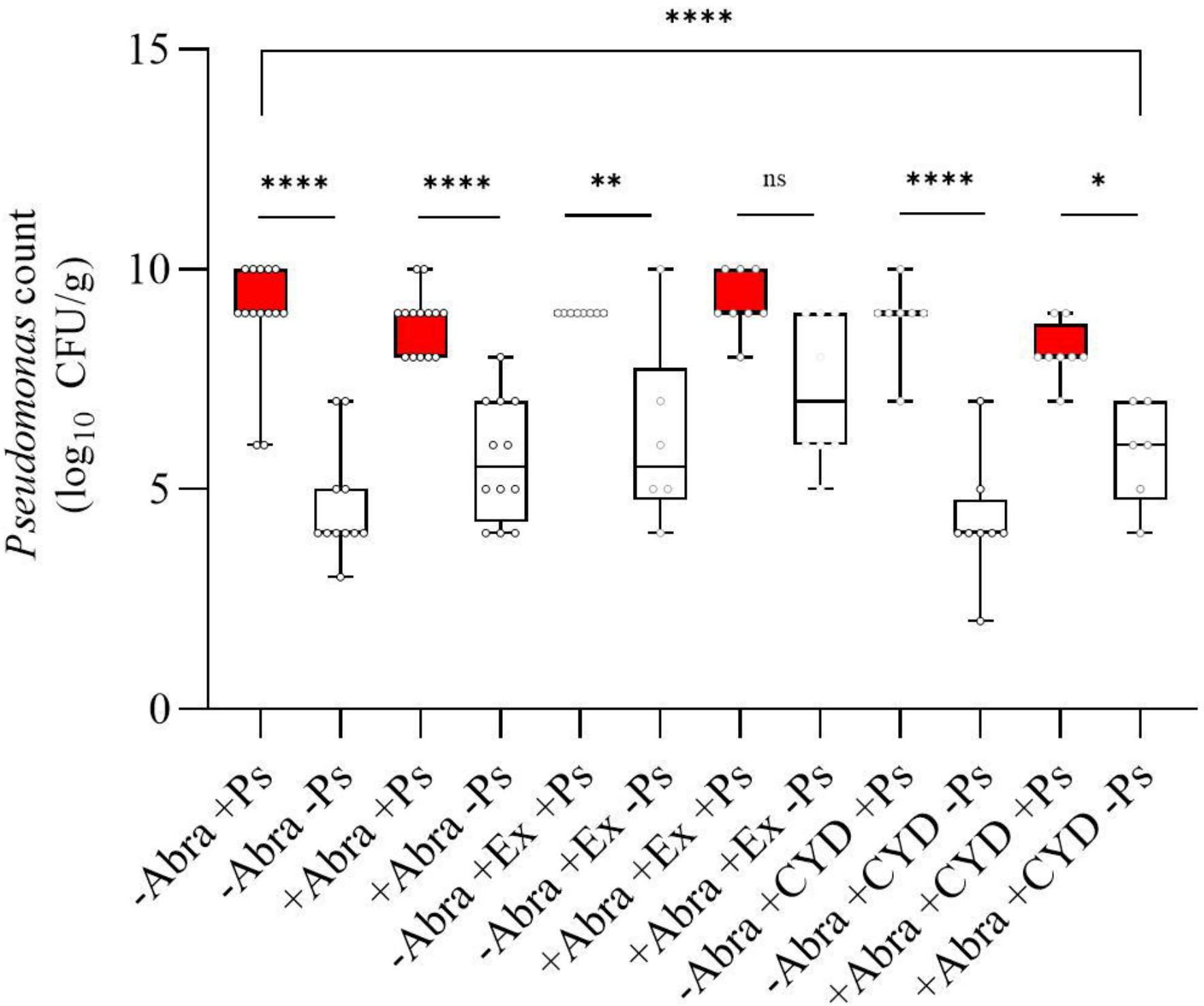
****
15
10
5
0
Pseudomonas count
(log10 CFU/g)
****
****
**
ns
****
*
-Abra +Ps
-Abra -Ps
+Abra +Ps
+Abra -Ps
-Abra +Ex +Ps
-Abra +Ex -Ps
+Abra +Ex +Ps
+Abra +Ex -Ps
-Abra +CYD +Ps
-Abra +CYD -Ps
+Abra +CYD +Ps
+Abra +CYD -Ps

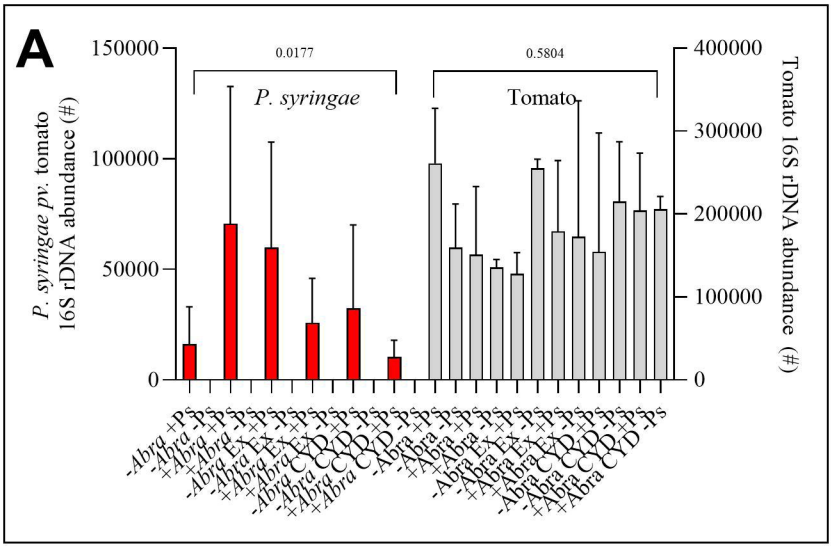
A
0.0177
0.5804
P. syringae
Tomato
P. syringae pv. tomato 16S rDNA abundance (#)
Tomato 16S rDNA abundance (#)
150000
100000
50000
0
400000
300000
200000
100000
0
-Abra +Ps
-Abra -Ps
+Abra +Ps
+Abra -Ps
-Abra +Ex +Ps
-Abra +Ex -Ps
+Abra +Ex +Ps
+Abra +Ex -Ps
-Abra +CYD +Ps
-Abra +CYD -Ps
+Abra +CYD +Ps
+Abra +CYD -Ps

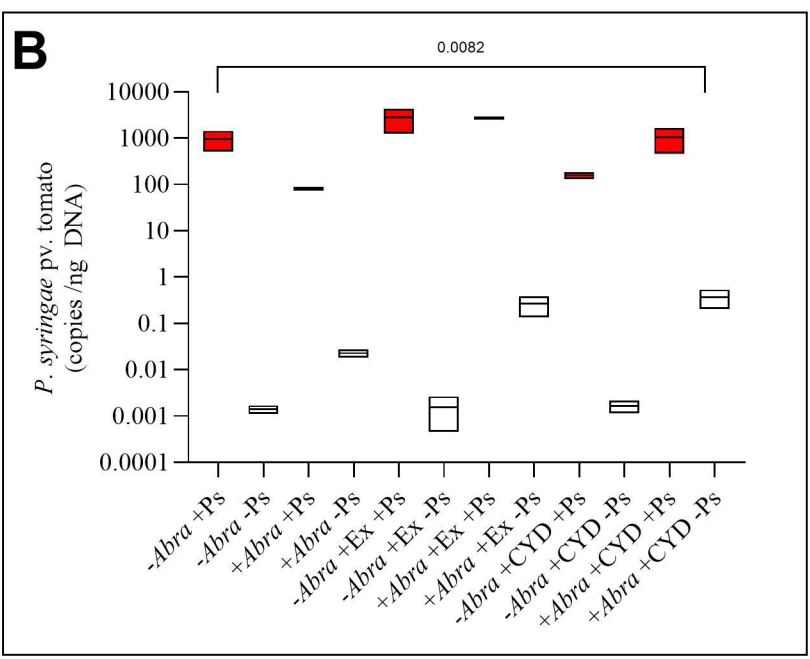
B
0.0082
P. syringae pv. tomato (copies /ng DNA)
10000
1000
100
10
1
0.1
0.01
0.001
0.0001
-Abra +Ps
-Abra -Ps
+Abra +Ps
+Abra -Ps
-Abra +Ex +Ps
-Abra +Ex -Ps
+Abra +Ex +Ps
+Abra +Ex -Ps
-Abra +CYD +Ps
-Abra +CYD -Ps
+Abra +CYD +Ps
+Abra +CYD -Ps

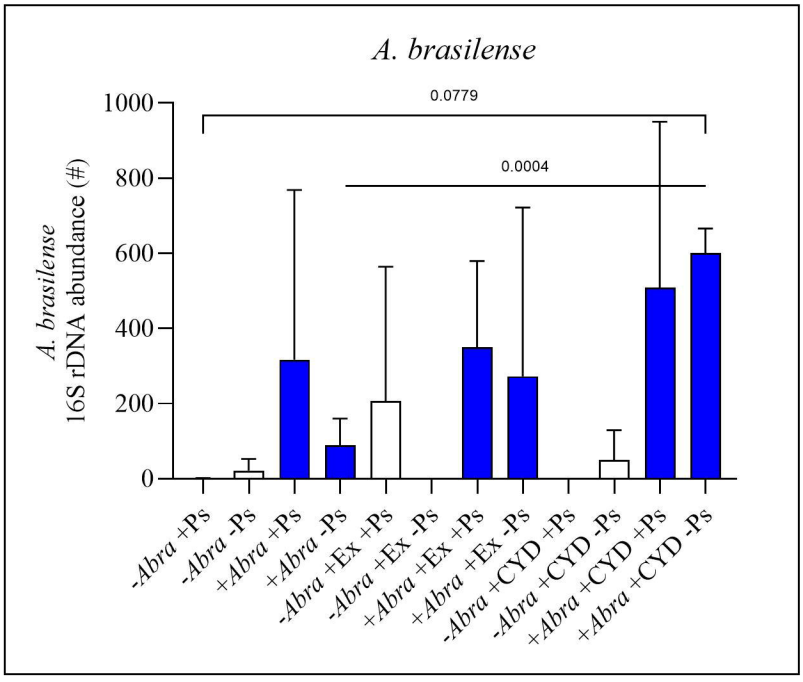
A. brasilense
0.0779
0.0004
1000
800
600
400
200
0
A. brasilense
16S rDNA abundance (#)
-Abra +Ps
-Abra -Ps
+Abra +Ps
+Abra -Ps
-Abra +Ex +Ps
-Abra +Ex -Ps
+Abra +Ex +Ps
+Abra +Ex -Ps
-Abra +CYD +Ps
-Abra +CYD -Ps
+Abra +CYD +Ps
+Abra +CYD -Ps

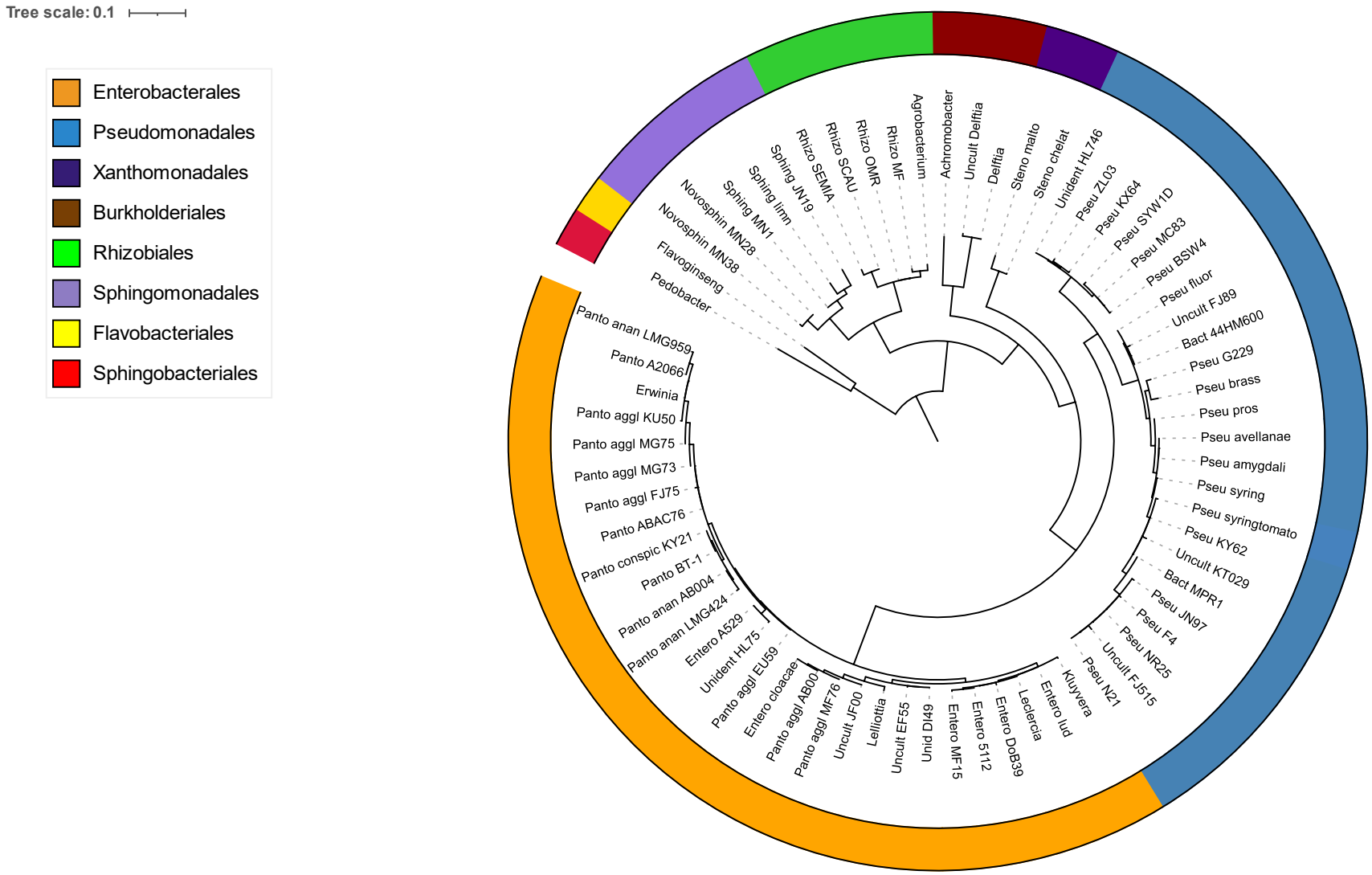
Tree scale: 0.1
Enterobacterales
Pseudomonadales
Xanthomonadales
Burkholderiales
Rhizobiales
Sphingomonadales
Flavobacteriales
Sphingobacteriales
Agrobacterium
Achromobacter
Uncult Delftia
Delftia
Steno malto
Steno chelat
Unident HL746
Pseu ZL03
Pseu KX64
Pseu SYW1D
Pseu MC83
Pseu BSW4
Pseu fluor
Uncult FJ89
Bact 44HM600
Pseu G229
Pseu brass
Pseu pros
Pseu avellanae
Pseu amygdali
Pseu syring
Pseu syringtomato
Pseu KY62
Uncult KT029
Bact MPR1
Pseu JN97
Pseu F4
Pseu NR25
Uncult FJ515
Pseu N21
Kluyvera
Entero lud
Leclercia
Entero DoB39
Entero 5112
Entero MF15
Unid DI49
Uncult EF55
Lelliottia
Uncult JF00
Panto aggl MF76
Panto aggl AB00
Entero cloacae
Panto aggl EU59
Unident HL75
Entero A529
Panto anan LMG424
Panto anan AB004
Panto BT-1
Panto conspic KY21
Panto ABAC76
Panto aggl FJ75
Panto aggl MG73
Panto aggl MG75
Panto aggl KU50
Erwinia
Panto A2066
Panto anan LMG959
Pedobacter
Flavoginseng
Novosphin MN38
Novosphin MN28
Sphing MN1
Sphing limn
Sphing JN19
Rhizo SEMIA
Rhizo SCAU
Rhizo OMR
Rhizo MF

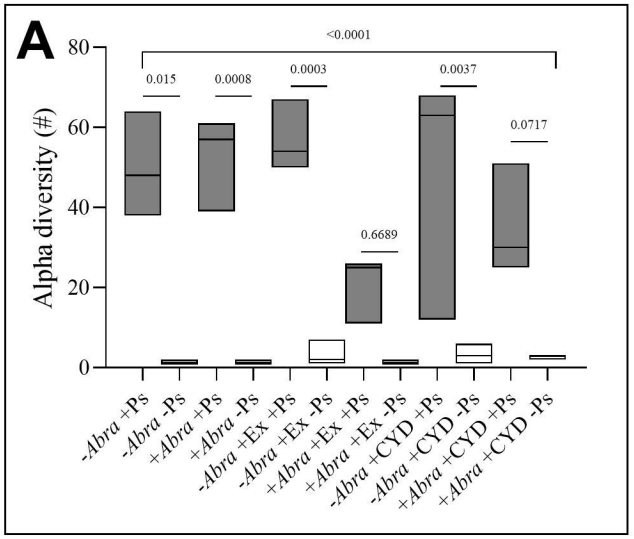
A
Alpha diversity (#)
<0.0001
0.015
0.0008
0.0003
0.6689
0.0037
0.0717
-Abra +Ps
-Abra -Ps
+Abra +Ps
+Abra -Ps
-Abra +Ex +Ps
-Abra +Ex -Ps
+Abra +Ex +Ps
+Abra +Ex -Ps
-Abra +CYD +Ps
-Abra +CYD -Ps
+Abra +CYD +Ps
+Abra +CYD -Ps

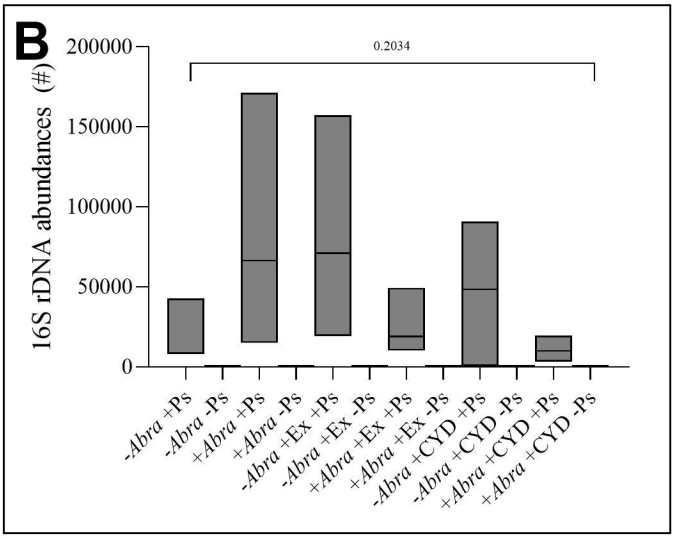
B
16S rDNA abundances (#)
0.2034
-Abra +Ps
-Abra -Ps
+Abra +Ps
+Abra -Ps
-Abra +Ex +Ps
-Abra +Ex -Ps
+Abra +Ex +Ps
+Abra +Ex -Ps
-Abra +CYD +Ps
-Abra +CYD -Ps
+Abra +CYD +Ps
+Abra +CYD -Ps

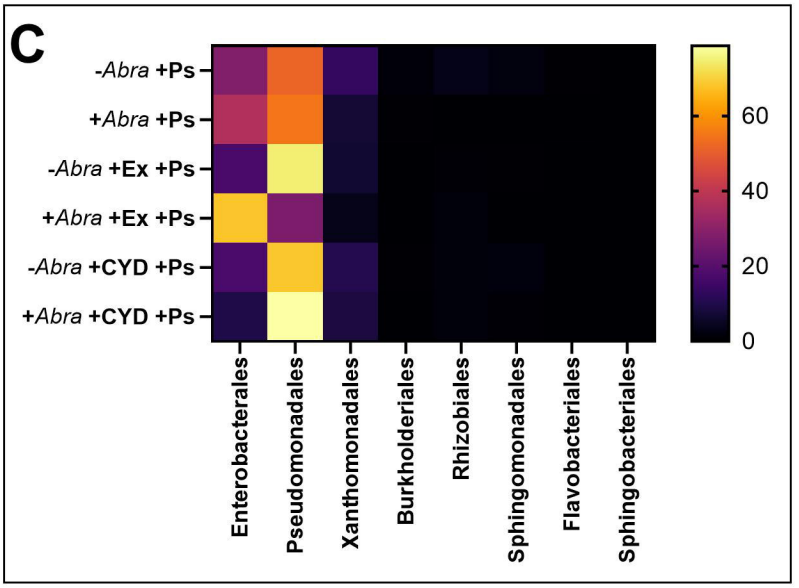
C
-Abra +Ps
+Abra +Ps
-Abra +Ex +Ps
+Abra +Ex +Ps
-Abra +CYD +Ps
+Abra +CYD +Ps
Enterobacterales
Pseudomonadales
Xanthomonadales
Burkholderiales
Rhizobiales
Sphingomonadales
Flavobacteriales
Sphingobacteriales

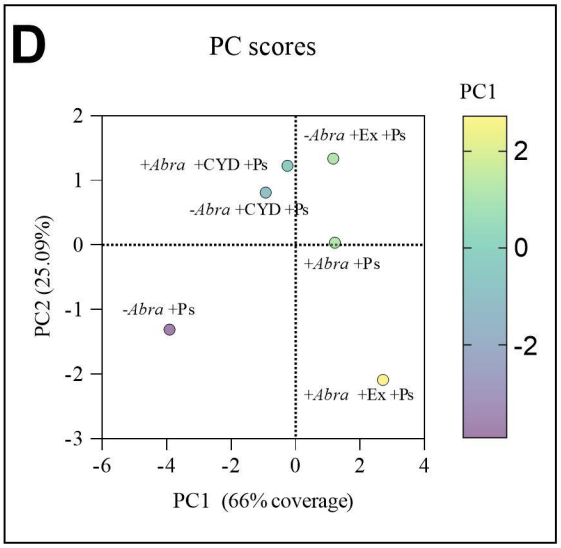
D
PC scores
PC1
-Abra +Ex +Ps
+Abra +CYD +Ps
-Abra +CYD +Ps
+Abra +Ps
-Abra +Ps
+Abra +Ex +Ps
PC2 (25.09%)
PC1 (66% coverage)

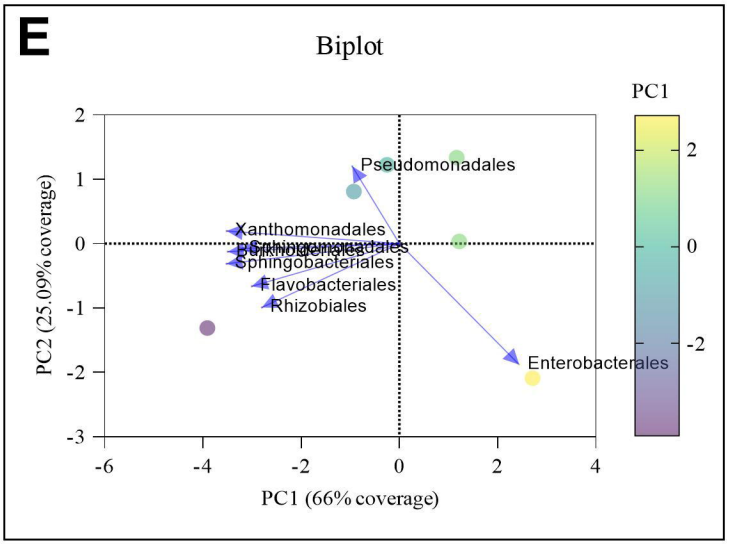
E
Biplot
PC1
Pseudomonadales
Xanthomonadales
Sphingobacteriales
Flavobacteriales
Rhizobiales
Enterobacterales
PC2 (25.09% coverage)
PC1 (66% coverage)

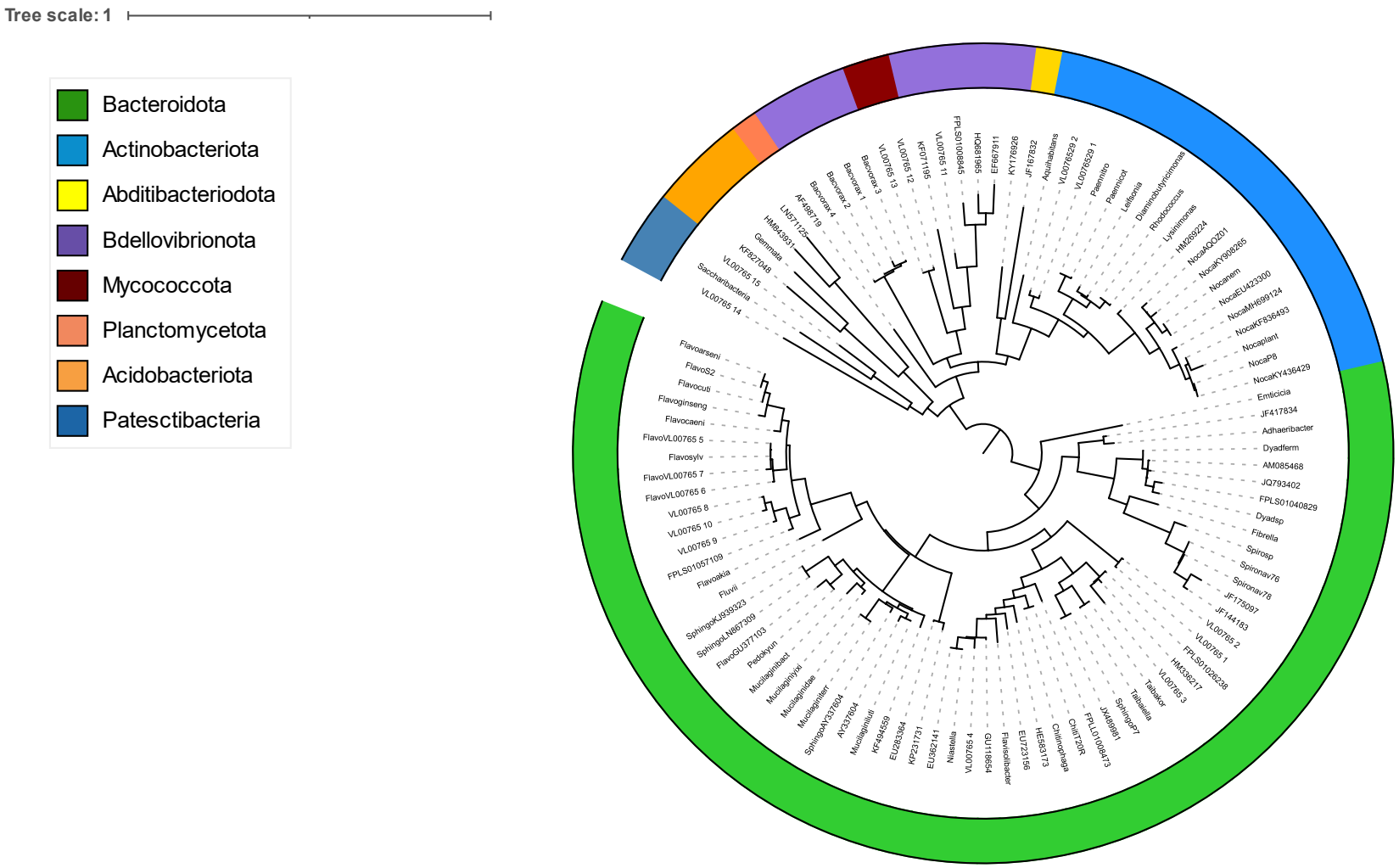
Tree scale: 1
Bacteroidota
Actinobacteriota
Abditibacteriodota
Bdellovibrionota
Mycococcota
Planctomycetota
Acidobacteriota
Patesctibacteria

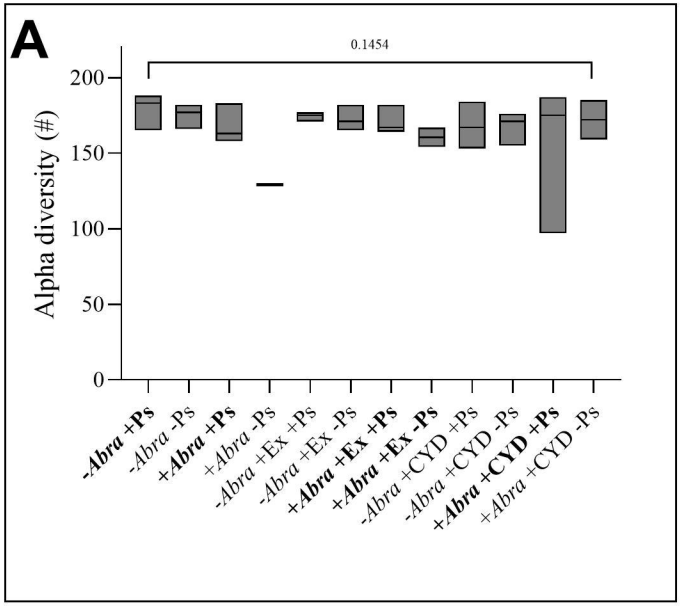
A
0.1454
Alpha diversity (#)
200
150
100
50
0
-Abra +Ps
-Abra -Ps
+Abra +Ps
+Abra -Ps
-Abra +Ex +Ps
-Abra +Ex -Ps
+Abra +Ex +Ps
+Abra +Ex -Ps
-Abra +CYD +Ps
-Abra +CYD -Ps
+Abra +CYD +Ps
+Abra +CYD -Ps

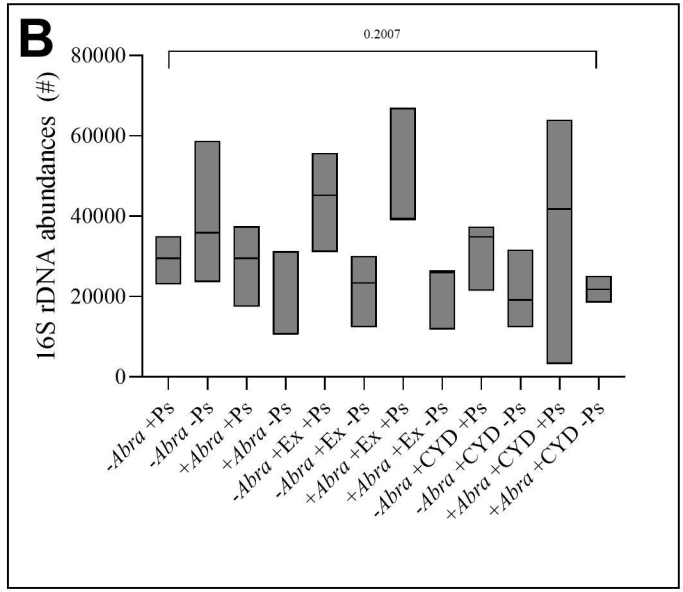
B
0.2007
16S rDNA abundances (#)
80000
60000
40000
20000
0
-Abra +Ps
-Abra -Ps
+Abra +Ps
+Abra -Ps
-Abra +Ex +Ps
-Abra +Ex -Ps
+Abra +Ex +Ps
+Abra +Ex -Ps
-Abra +CYD +Ps
-Abra +CYD -Ps
+Abra +CYD +Ps
+Abra +CYD -Ps

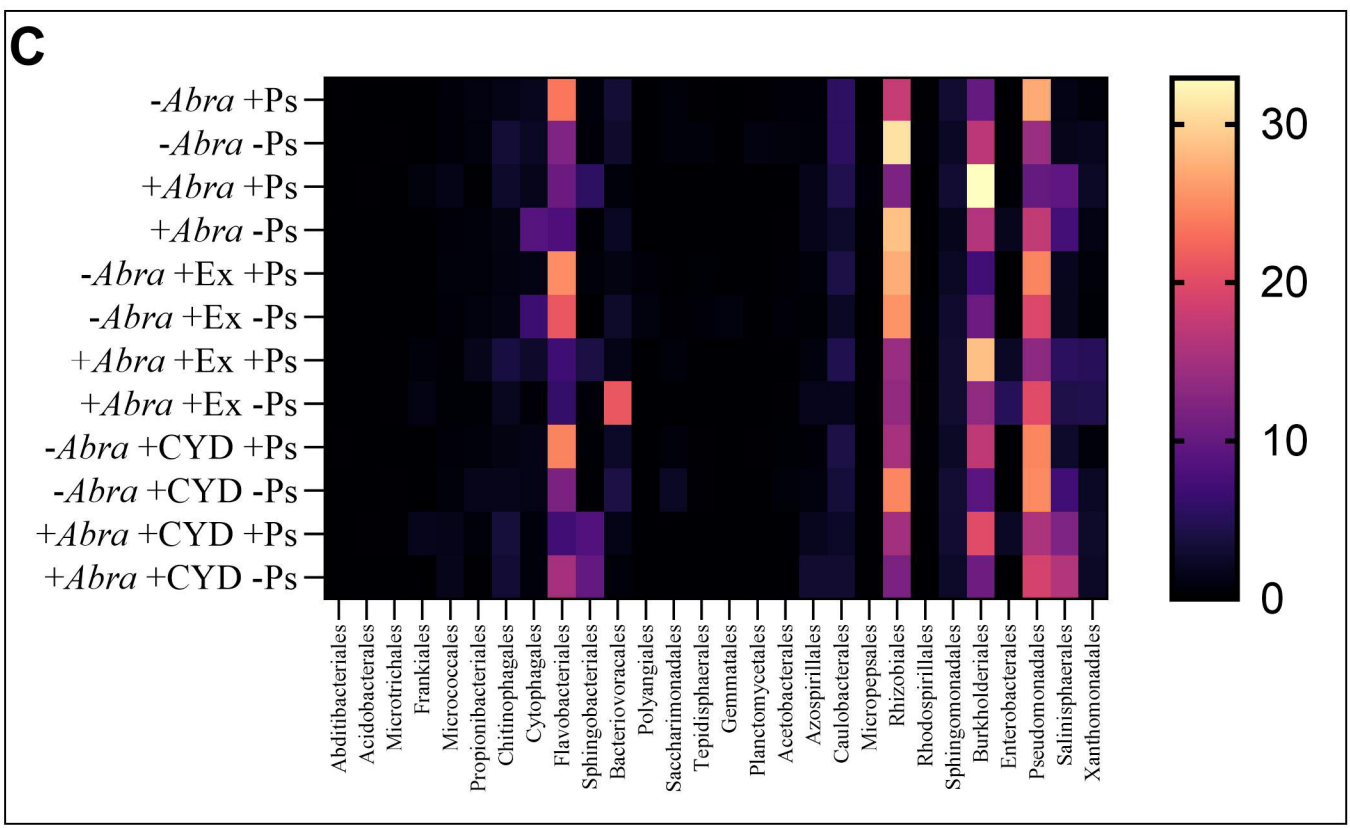
C
-Abra +Ps
-Abra -Ps
+Abra +Ps
+Abra -Ps
-Abra +Ex +Ps
-Abra +Ex -Ps
+Abra +Ex +Ps
+Abra +Ex -Ps
-Abra +CYD +Ps
-Abra +CYD -Ps
+Abra +CYD +Ps
+Abra +CYD -Ps
Abditibacteriales
Acidobacterales
Microtrichales
Frankiales
Micrococcales
Propionibacteriales
Chitinophagales
Cytophagales
Flavobacteriales
Sphingobacteriales
Bacteriovoracales
Polyangiales
Saccharimonadales
Tepidisphaerales
Gemmatales
Planctomycetales
Acetobacterales
Azospirillales
Caulobacterales
Micropepsales
Rhizobiales
Rhodospirillales
Sphingomonadales
Burkholderiales
Enterobacterales
Pseudomonadales
Salinisphaerales
Xanthomonadales
30
20
10
0

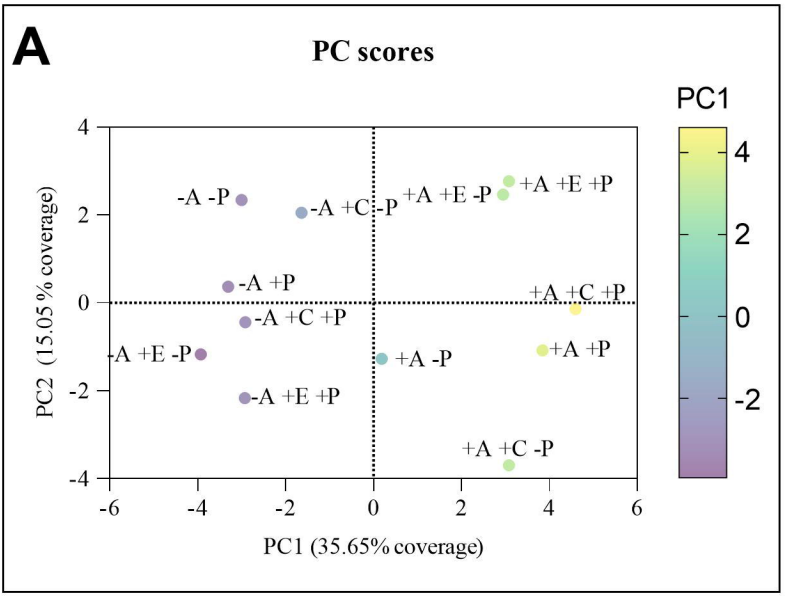
A
PC scores
PC1
-A -P
-A +C -P
+A +E -P
+A +E +P
-A +P
+A +C +P
-A +C +P
-A +E -P
+A -P
+A +P
-A +E +P
+A +C -P
PC2 (15.05 % coverage)
PC1 (35.65% coverage)

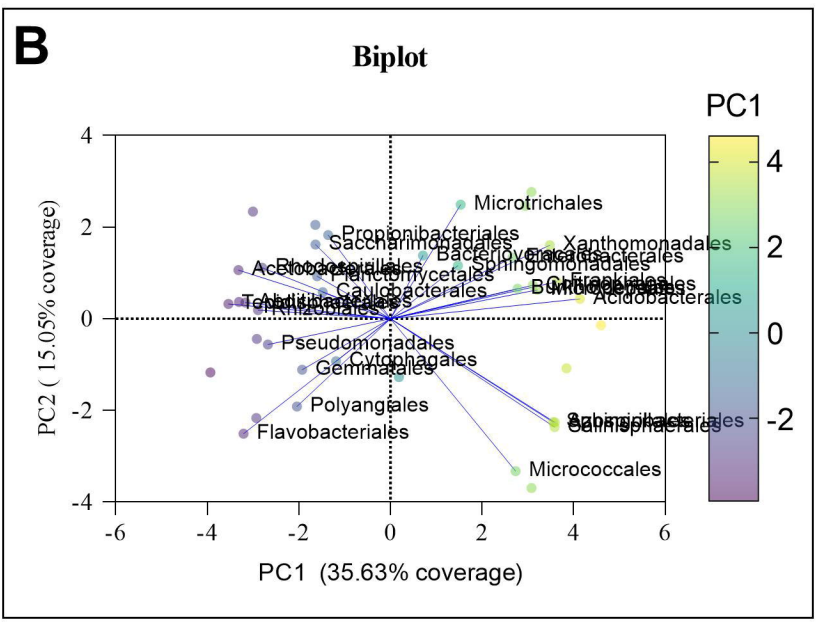
B
Biplot
PC1
Microtrichales
Propionibacteriales
Saccharimonadales
Xanthomonadales
Acidobacterales
Caulobacterales
Pseudomonadales
Cytophagales
Gemmatales
Polyangiales
Flavobacteriales
Micrococcales
PC2 (15.05% coverage)
PC1 (35.63% coverage)

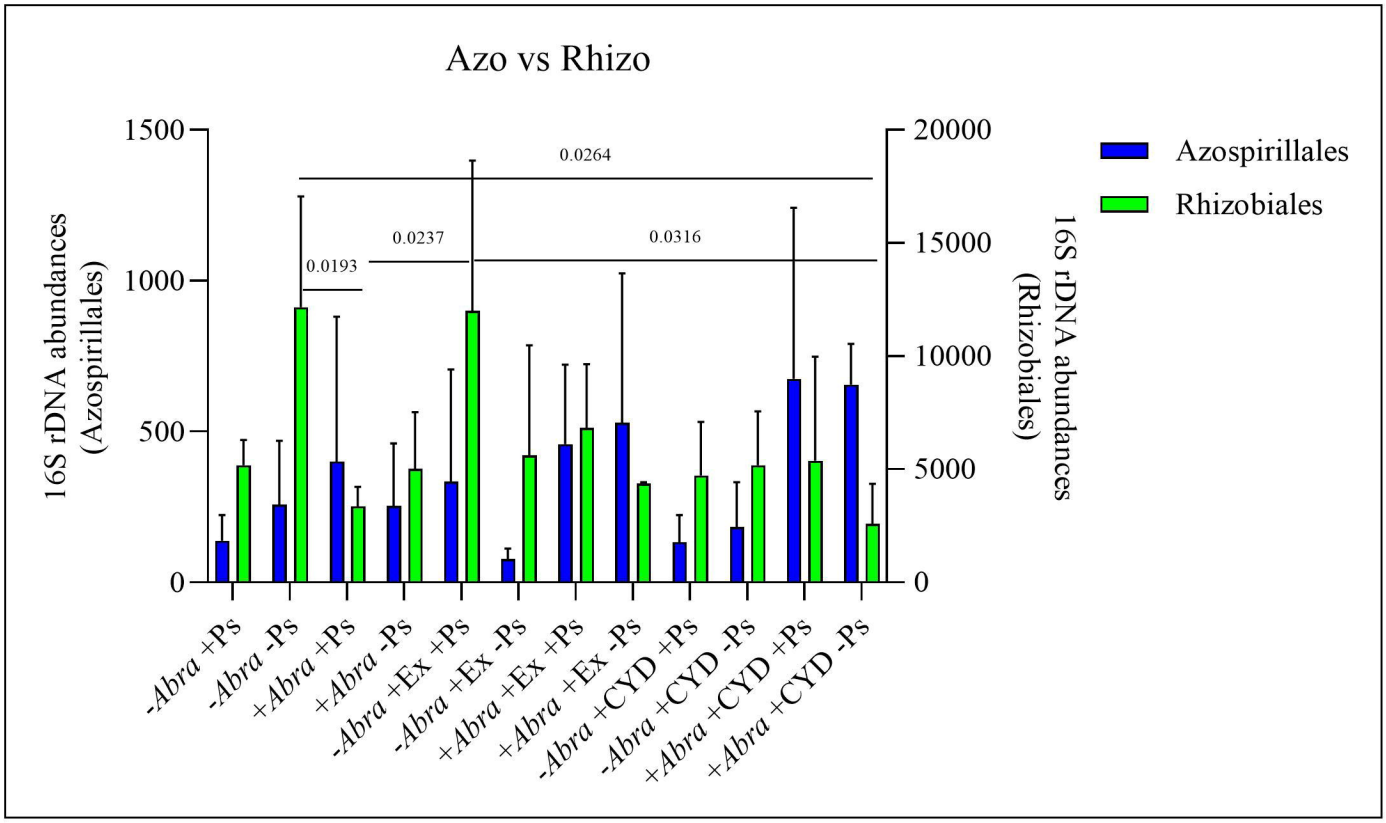
Azo vs Rhizo
16S rDNA abundances (Azospirillales)
16S rDNA abundances (Rhizobiales)
1500
1000
500
0
20000
15000
10000
5000
0
0.0264
0.0237
0.0316
0.0193
Azospirillales
Rhizobiales
-Abra +Ps
-Abra -Ps
+Abra +Ps
+Abra -Ps
-Abra +Ex +Ps
-Abra +Ex -Ps
+Abra +Ex +Ps
+Abra +Ex -Ps
-Abra +CYD +Ps
-Abra +CYD -Ps
+Abra +CYD +Ps
+Abra +CYD -Ps